

See discussions, stats, and author profiles for this publication at: <https://www.researchgate.net/publication/279940933>

The Ilímaussaq Alkaline Complex, South Greenland

Chapter · May 2015

DOI: 10.1007/978-94-017-9652-1_14

CITATIONS

46

READS

2,526

1 author:



Michael A W Marks

University of Tuebingen

135 PUBLICATIONS 3,399 CITATIONS

SEE PROFILE

Some of the authors of this publication are also working on these related projects:



Multi-aquifer fluid mixing processes as first order processes for ore precipitation [View project](#)



Chemical evolution of continental basement brines - constraints using fluid inclusion analyses [View project](#)

Chapter 14

The Ilímaussaq Alkaline Complex, South Greenland

Michael A. W. Marks and Gregor Markl

Abstract The Ilímaussaq complex in South Greenland is a well-studied multiphase alkaline to peralkaline intrusion of Mesoproterozoic age. Most of the Ilímaussaq rocks are extremely enriched in alkalis, iron, halogens, high-field-strength elements (HFSE) and other rare elements, forming one of the most differentiated peralkaline rock suites known.

The major factors causing the extreme differentiation trends are low oxygen fugacity and silica activity as well as very low water activity in the melts. These inhibit the early exsolution of aqueous NaCl-bearing fluids and facilitate the enrichment of alkalis and halogens in the melts, thereby increasing the solubility of HFSE. The unusually long crystallization interval of these rocks and the suspected continuous transition from melt to fluid results in extensive (auto)metasomatism and hydrothermal overprint. Primary mineral assemblages are therefore partially resorbed in most rock units and replaced by secondary minerals to various extents.

The Ilímaussaq complex is a well-known example of magmatic layering in peralkaline plutonic rocks. Recent investigations of mineral chemical trends in the layered rocks permit better understanding of their formation. The mechanism of crystal mats formation in the cooling magma causing crowding effects during settling of the layering-forming minerals is believed to govern the formation of the Ilímaussaq layered sequence.

Despite more than 100 years of research and hundreds of publications on Ilímaussaq, important aspects on the origin of some Ilímaussaq rocks, the architecture and deep structure of the complex and the significance of hydrocarbons and bitumens present in the peralkaline rocks remain unclear. Thus, plenty of room for further studies on these unusual rocks exists and interdisciplinary research is needed to better understand the genesis of this unique magmatic complex.

Keywords Peralkaline rocks · Agpaitic rocks · Eudialyte · Oxygen fugacity · Halogens · Metasomatism

M. A. W. Marks (✉) G. Markl
Mathematisch-Naturwissenschaftliche Fakultät, FB Geowissenschaften,
Universität Tübingen, Wilhelmstrasse 56, 72074 Tübingen, Germany
e-mail: michael.marks@uni-tuebingen.de

© Springer Science+Business Media Dordrecht 2015
B. Charlier et al. (eds.), *Layered Intrusions*, Springer Geology,
DOI 10.1007/978-94-017-9652-1_14

649

Table 14.1 Overview on the less common minerals found in the Ilímaussaq complex. Minerals for which the Ilímaussaq complex is the type locality are marked in italic, asterisks mark minerals, which have not been described from other localities. For a full list of minerals identified in the Ilímaussaq alkaline complex, the reader is referred to Petersen (2001).

Aegirine	$\text{NaFeSi}_2\text{O}_6$
<i>Aenigmatite</i>	$\text{Na}_2\text{Fe}_5\text{TiSi}_6\text{O}_{20}$
Analcime	$\text{NaAlSi}_2\text{O}_6 \cdot \text{H}_2\text{O}$
<i>Arfvedsonite</i>	$\text{Na}_3\text{Fe}_5\text{Si}_8\text{O}_{22}(\text{OH})_2$
Astrophyllite	$(\text{K}, \text{Na})_3(\text{Fe}, \text{Mn})_7\text{Ti}_2\text{Si}_8\text{O}_{24}(\text{O}, \text{OH})_7$
Baddeleyite	ZrO_2
Catapleite	$\text{Na}_2\text{ZrSi}_3\text{O}_9 \cdot 2\text{H}_2\text{O}$
Chkalovite	$\text{NaBeSi}_2\text{O}_6$
Djerfisherite	$\text{K}_6(\text{Fe}, \text{Cu}, \text{Ni})_{25}\text{S}_{26}\text{Cl}$
Elpidite	$\text{Na}_2\text{ZrSi}_6\text{O}_{15} \cdot 3\text{H}_2\text{O}$
Epididymite	$\text{Na}_2\text{Be}_2\text{Si}_6\text{O}_{15} \cdot \text{H}_2\text{O}$
<i>Eudialyte</i>	$\text{Na}_{15}\text{Ca}_6\text{Fe}_3\text{Zr}_3\text{Si}_{26}\text{O}_{73}(\text{O}, \text{OH}, \text{H}_2\text{O})_3(\text{Cl}, \text{OH})_2$
Murmanite	$\text{Na}_2(\text{Ti}, \text{Nb})_2\text{Si}_2\text{O}_9 \cdot 2\text{H}_2\text{O}$
Natrosilite	$\text{Na}_2\text{Si}_2\text{O}_5$
Natrophosphate	$\text{Na}_7(\text{PO}_4)_2\text{F} \cdot 19 \text{H}_2\text{O}$
<i>Naujakasite*</i>	$\text{Na}_6(\text{Fe}, \text{Mn})\text{Al}_4\text{Si}_8\text{O}_{26}$
Neptunite	$\text{KNa}_2\text{Li}(\text{Fe}, \text{Mg}, \text{Mn})_2\text{Ti}_2\text{Si}_8\text{O}_{24}$
Pyrochlore	$(\text{Na}, \text{Ca})_2\text{Nb}_2(\text{O}, \text{OH}, \text{F})_7$
<i>Rinkite</i>	$(\text{Na}, \text{Ca})_3(\text{Ca}, \text{REE})_4\text{TiSi}_4\text{O}_{15}\text{F}_3$
<i>Sodalite</i>	$\text{Na}_8(\text{Al}_6\text{Si}_6\text{O}_{24})\text{Cl}_2$
<i>Sørensenite*</i>	$\text{Na}_4\text{Be}_2\text{Sn}(\text{Si}_3\text{O}_9)_2 \cdot 2 \text{H}_2\text{O}$
<i>Steenstrupine</i>	$\text{Na}_{14}\text{Mn}_2(\text{Fe}, \text{Mn})_2\text{REE}_6\text{ZrSi}_{12}\text{O}_{36}(\text{PO}_4)_7 \cdot 3\text{H}_2\text{O}$
Thermonatrite	$\text{Na}_2\text{CO}_3 \cdot \text{H}_2\text{O}$
Trona	$\text{Na}_3(\text{HCO}_3)(\text{CO}_3) \cdot 2\text{H}_2\text{O}$
<i>Tugtupite</i>	$\text{Na}_4(\text{AlBeSi}_4\text{O}_{12})\text{Cl}$
<i>Ussingite</i>	$\text{Na}_2\text{AlSi}_3\text{O}_8\text{OH}$
Villiaumite	NaF

Introduction

The Ilímaussaq igneous complex in South Greenland is a Mesoproterozoic composite intrusion that mainly consists of syenitic and nepheline syenitic rocks. It is the type locality of agpaite rocks, which are peralkaline (molar $(\text{Na} + \text{K})/\text{Al} > 1$) rocks containing complex $\text{Na}-\text{Ca}-(\text{Ti}, \text{Zr})$ -silicates, the most common being eudialyte-group minerals (Sørensen 1997; Marks et al. 2011, see Table 14.1 for mineral formulae). To date, it is believed that such rock types form by fractional crystallization processes of alkali basaltic and nephelinitic parental magmas derived from lithospheric mantle sources (Larsen and Sørensen 1987; Kramm and Kogarko 1994;

Marks et al. 2011; Schilling et al. 2011). In that sense, the Ilímaussaq rocks are some of the most extreme products of magmatic differentiation processes known. As a consequence, they comprise some of the most unusual magmatic rock types—both in terms of mineralogy and geochemistry (Table 14.2).

The agpaitic rocks of the complex are highly enriched in alkalis (Li, Na, Rb, Cs), halogens (F, Cl, Br, I), high field strength elements (HFSE) such as Zr, Hf, Nb, Ta, REE, U, Th, and otherwise relatively rare elements such as Be, Sn, Sb, W, Mo, As, Zn, Pb and Ga (Bailey et al. 2001). It is therefore unsurprising that the complex is the type locality for some thirty minerals, some of which like sodalite, arfvedsonite and eudialyte occur as major rock-forming components; about ten minerals have only been found in the Ilímaussaq complex so far (Petersen 2001; Table 14.1). Consequently the area remains a magnet for mineral collectors as well as petrologists, mineralogists and geochemists and has given rise to several hundred publications to date.

Despite its exotic petrology, the Ilímaussaq complex can serve as a text-book example for studying a range of magmatic and hydrothermal processes. Because of its exceptionally long crystallization interval and the major changes in the mineralogy of the successive rock units, the complex offers a unique possibility to study the stability relations and compositional evolution of rock-forming minerals in alkaline to peralkaline magmas and the parameters governing the enrichment of Na, Fe, halogens, HFSE and other rare elements in such systems (e.g., Larsen 1976; Markl et al. 2001; Markl and Baumgartner 2002; Andersen and Sørensen 2005; Graser and Markl 2008; Marks et al. 2011).

Some Ilímaussaq rocks have economically very attractive levels of REE, Zr, Nb, Be and U. The complex has therefore a long prospection and exploration history (Sørensen 1992, 2001). Recent developments on the REE market as well as political changes in Greenland has led to increased exploration activity in the complex and the Ilímaussaq complex hosts some of the largest deposits of REEs and U worldwide (Parsons 2012; GMEL 2015; TANBREEZ 2014).

Igneous layering is another characteristic of most Ilímaussaq rocks. In general, igneous layering is a common feature in large mafic and ultramafic intrusions. Some of the most famous localities are Skaergaard in Greenland, Rum in the UK, Stillwater in the USA, Kiglapait in Canada, Bushveld in South Africa and the Great Dyke in Zimbabwe (e.g., McBirney 1996; Emeleus et al. 1996; McCallum 1996; Morse 1969; Eales and Cawthorn 1996; Wilson 1996). Whilst magmatic layering in granitic complexes is relatively rarely described (e.g., Dolbel in Niger, Pupier et al. 2008; High Tatra in Poland, Gaweda and Szopa 2011) it is a phenomenon quite commonly encountered in syenitic intrusions. Well-known examples occur in the Kola peninsula, Russia (Vlasov et al. 1966; Sørensen 1968; Féménias et al. 2005; Galakhov 1975; Kramm and Kogarko 1994; Arzamastsev et al. 1998) as well as in the Gardar Province, South Greenland (see Upton et al. 1996 for a review) including the Ilímaussaq complex. In the latter, the most spectacular example is exhibited by the so-called kakortokite-lujavrite sequence (see Table 14.2 for the major Ilímaussaq rock units). However, the origin of this layered sequence and its relation to the other Ilímaussaq rocks is still not satisfactorily explained.

Table 14.2 Overview on the major rock types of the Ilmaussaq complex (Partly adapted from Sørensen 2006).

Rock type	Texture	Major minerals	Minor minerals
Augite syenite	Medium- to coarse-grained, hypidiomorphic to xenomorphic granular, massive or layered	Alkali feldspar, olivine, Ca-rich augite (diopside to hedenbergite), titanomagnetite, calcic amphibole (ferro-edomite-ferro-pargasite-hastingsite)	Nepheline, biotite, apatite, baddeleyite/zircon, pyrrhotite, chalcopyrite, sphalerite, galena
Pulaskite and foyaite	Medium- to coarse-grained, massive	Alkali feldspar, nepheline, olivine, hedenbergite to aegirine, sodic-calcic to sodic amphibole (katophorite to arfvedsonite)	Titanomagnetite, apatite, biotite, aenigmatite, fluorite, eudialyte, analcime, pyrrhotite, sphalerite, galena and others
Sodalite foyaite	Coarse-grained, foyaitic	Alkali feldspar, nepheline, sodalite, hedenbergite to aegirine, katophorite-arfvedsonite	Olivine, titanomagnetite, apatite, biotite, aenigmatite, fluorite, eudialyte, analcime, pyrrhotite, sphalerite, galena, djerfisherite and others
Naujaite	Coarse-grained to pegmatitic, poikilitic, massive and layered	Alkali feldspar, nepheline, sodalite, hedenbergite to aegirine, katophorite-arfvedsonite, eudialyte	Olivine, titanomagnetite, apatite, biotite, aenigmatite, fluorite/villiaumite, pectolite, pyrrhotite, sphalerite, galena, djerfisherite and others
Kakortokite	Mostly medium- to coarse-grained, mostly laminated and layered	Alkali feldspar, nepheline, eudialyte, sodic amphibole (arfvedsonite)	Sodalite, fluorite, aegirine, aenigmatite, rinkite, pyrrhotite, galena, sphalerite, native Sn and Pb and others
Lujavrite	Mostly medium- to fine-grained, mostly laminated	Albite, microcline, nepheline, sodalite, analcime, aegirine, arfvedsonite, eudialyte	Villiaumite, steenstrupine, naujakasite, sphalerite, galena, native Pb and many others. Depending on the respective Lujavrite type, some of these minerals (e.g., naujakasite) may be major constituents
Peralkaline granite and quartz syenites	Medium- to coarse-grained, hypidiomorphic granular	Alkali feldspar, quartz, arfvedsonite, aegirine	Aenigmatite, astrophyllite, elpidite, epididymite, zircon, ilmenite, fluorite, pyrochlore, sphalerite and others

Here we present an overview of the present understanding on the origin and evolution of the Ilímaussaq magmatic system. Furthermore, based on detailed mineral chemical investigations and structural data, we provide a new hypothesis on the origin of the kakortokite-lujavrite sequence of the complex. Finally, potential directions for further research aimed at a better understanding of this unique system are proposed.

Geological Setting of the Ilímaussaq Complex

The Ilímaussaq complex is part of the Gardar province in South Greenland, which represents an uplifted and eroded continental rift province of Mesoproterozoic age (see Upton et al. 2003 and Upton 2013 for recent reviews). During the early stages of rifting, between 1350 and 1140 Ma, a thick (~3500 m) sequence of lavas and sediments called Eriksfjord Formation accumulated (Poulsen 1964; Larsen 1977a; Halama et al. 2003). A large number of dykes and several mostly composite complexes intruded into a mainly Paleoproterozoic and subordinately Archean basement. The Paleoproterozoic basement country rocks for much of the Gardar Province consist of calc-alkaline granitoids composing the Andean-type Julianehåb batholith that developed within the Ketilidian orogenic belt. The batholith formed between 1850 and 1725 Ma and is considered to have originated following subduction of an oceanic plate beneath the Archean craton to the North (Garde et al. 2002). In the northwestern part of the province, Archean high-grade gneisses form the country rocks for some of the Gardar intrusives (Allaart 1976). Major dyke swarms were emplaced into the Julianehåb batholith mainly in the Tuttutooq-Ilímaussaq-Narsarsuaq and the Nunarsuit-Isortoq zones. They span a wide compositional range from basaltic to trachytic, phonolitic, rhyolitic, lamprophyric and carbonatitic (e.g., Upton and Emeleus 1987; Goodenough et al. 2002; Halama et al. 2004; Köhler et al. 2009). Anorthositic xenoliths of up to 100 m size occur frequently in some of the mafic and intermediate intrusions (Bridgwater and Harry 1968). It is therefore assumed that a large anorthositic complex may be present at depth underlying the whole province (Bridgwater and Harry 1968; Upton et al. 2003). A detailed study of plagioclase zonation in megacrysts allied to the anorthosites indicates crystallization at about 10–12 kbar prior to a rapid ascent to upper crustal levels (Halama et al. 2002). Some of the dykes, referred to as giant dykes on account of their widths of up to 800 m, are largely composed of coarse-grained gabbro (Bridgwater and Coe 1970). Where they are composite, the dykes have gabbroic margins and syenitic to alkali granitic centres (Upton and Emeleus 1987; Halama et al. 2004).

Several larger central-type plutonic complexes intruded into shallow crustal levels. Their depth of intrusion was approximately 2–5 km and it is likely that many of them had surface expressions (Emeleus and Upton 1976; Upton et al. 1990). They are often composite and the most common rock types are quartz syenite, syenite and nepheline syenite with subordinate alkali granite, gabbro and carbonatite. Most of the complexes contain layered cumulates and give evidence for strong in

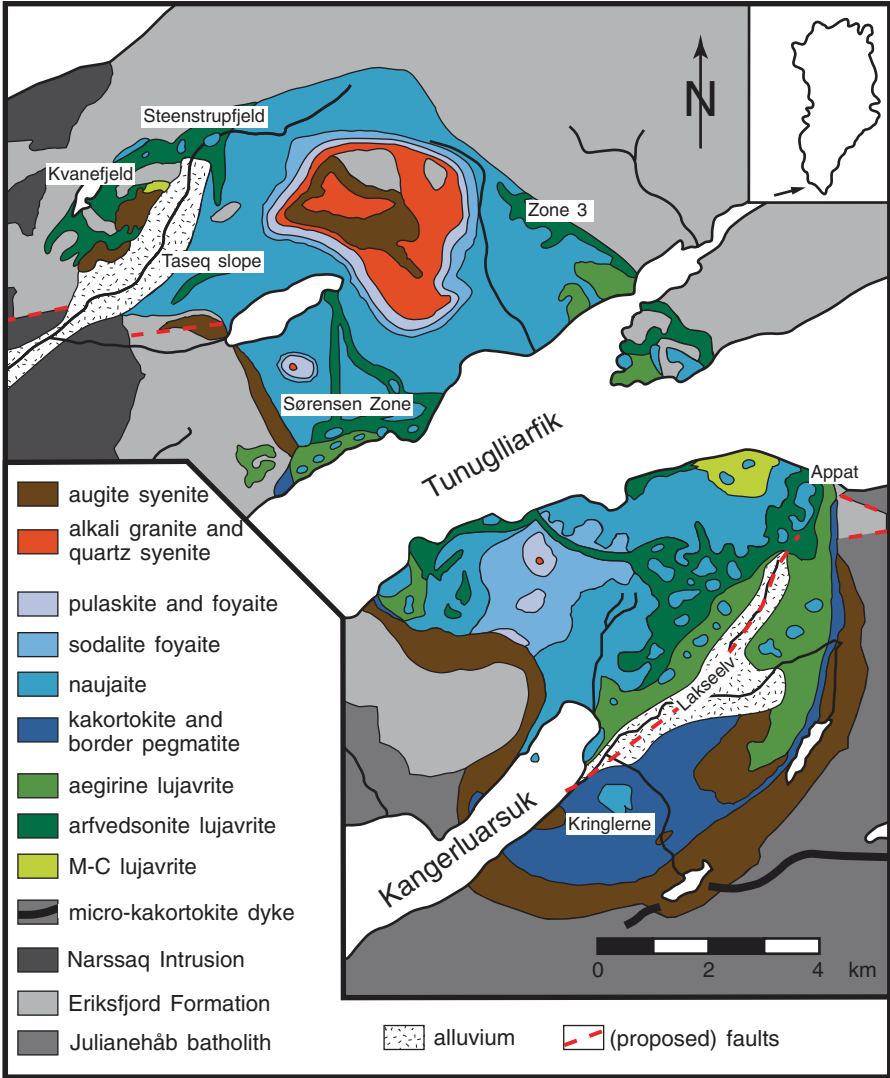


Fig. 14.1 Simplified geological map of the Ilímaussaq complex, South Greenland (Modified after Ferguson 1964 and Sørensen 2001).

situ fractional crystallization (Upton et al. 1996). Some of the complexes are silica-undersaturated and some are wholly oversaturated, which was probably controlled by the amount of crustal contamination experienced by the parental magmas (e.g., Stevenson et al. 1997; Marks et al. 2003, 2004). Unlike most other Gardar intrusions, the Ilímaussaq complex comprises both quartz-bearing and nepheline-bearing rocks, although the latter largely dominate (Fig. 14.1).

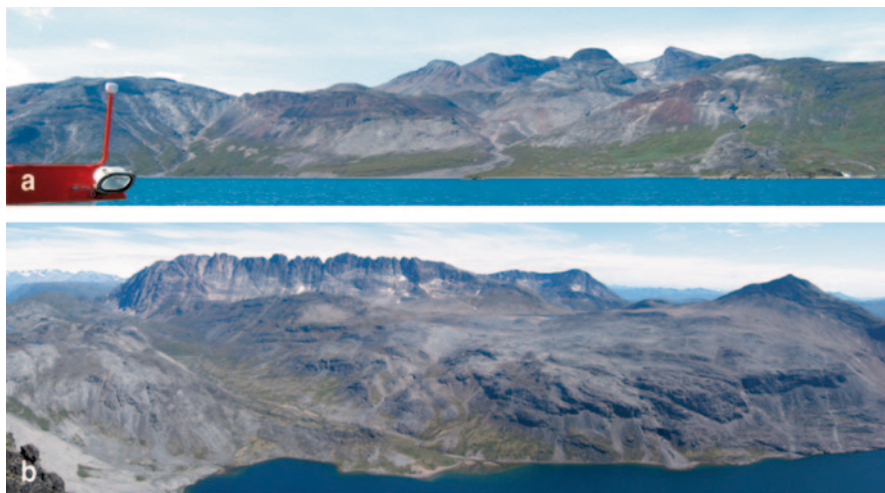


Fig. 14.2 Overview photographs of the Ilímaussaq complex. **a** The northern part of the complex as seen from the Tunulliarfik fjord towards the north. On the right side of the image, the contact between the Ilímaussaq rocks (*mostly light gray*) and the basaltic country rocks (*green from vegetation*) is clearly visible. The horizontal *dark gray top* of the mountain *right* of the *center* of the image is a large xenolith of basalt (compare Fig. 14.1). The red weathered areas are zones of intense oxidation. **b** The southern part of the complex with the Kangerluarsuk fjord in the foreground, view to the south. Note the brownish rim of augite syenite, which separates the layered kakortokite sequence from the mountainous granitoid basement rocks in the background. The *light gray rocks* in the *left* part of the picture are naujaites, which are separated from the kakortokites to the right by slightly darker lujavrites.

Field Relations among Major Rock Types and General Structure of the Complex

The complex has an ovoid plan measuring 18 by 8 km. Its location was structurally controlled, and emplacement of the Ilímaussaq magma(s) is considered to have been by block subsidence and stoping (Ussing 1912; Ferguson 1964; Sørensen 1978). The northern part of the complex exposes the roof region of the Ilímaussaq magma chamber and intrudes the volcano-sedimentary succession of the Eriksfjord Formation. In contrast, a stratigraphically lower level is exposed in the southern part of the complex in which the contacts of the Ilímaussaq rocks are against the granitic country rocks beneath the unconformity with the Eriksfjord Formation (Figs. 14.1 and 14.2).

Several major intrusive phases can be distinguished in the complex: (1) met-aluminous augite syenite, (2) peralkaline granite and quartz syenite and (3) peralkaline nepheline syenites. Most of the latter contain eudialyte-group minerals, mineralogically classifying them as agpaitic rocks (e.g., Ussing 1912; Sørensen 1997; Marks et al. 2011). The nepheline syenites largely dominate the complex

and are subdivided into (i) coarse-grained roof series (pulaskite, foyaite, sodalite foyaite, naujaite) and floor series (kakortokite) cumulate rocks and (ii) several types of mostly fine-grained and melanocratic rocks (lujavrites), many of which possess strong magmatic fabrics. The lujavrites intrude the roof series rocks, but not the floor series cumulates. Detailed petrographic descriptions of the major Ilímaussaq rocks are presented in Ussing (1912), Ferguson (1964) and Hamilton (1964). Here we present only a brief summary, Table 14.2 and Fig. 14.3 give an overview of the textures and mineralogy of the major Ilímaussaq rocks.

The oldest unit of the complex is augite syenite. It consists of perthitic alkali feldspar, fayalitic olivine, Ca-rich augite (diopside to hedenbergite), Fe–Ti oxides (ulvöspinel-rich magnetite \pm ilmenite) and calcic amphibole (hastingsite to ferropargasite to ferro-edenite), with minor amounts of nepheline, biotite, apatite, zircon/baddeleyite and various sulphides (Ferguson 1964; Larsen 1976; Karup-Møller 1978; Marks and Markl 2001; Fig. 14.3a). In the southern part of the complex, it occurs as a nearly continuous shell with variable thicknesses between about 10 and 1000 m (Fig. 14.1). The augite syenite is relatively fine-grained at its contacts towards the Julianehåb granitoids and its grain size increases towards the agpaitic rocks. An increase in the modal amount of interstitial nepheline as well as systematic changes in the composition of olivine and augite from the margins inwards imply that the augite syenite crystallized inwards perpendicular to this contact (Larsen 1976; Marks and Markl 2001). Rafts of augite syenite (up to tens of metres across) occur within the agpaitic rocks. In places these are surrounded by up to 2 m thick pegmatites and show variable signs of fluid-induced interaction with their host rocks (Schönenberger et al. 2006). In the northern part of the complex, the augite syenite envelope is largely missing except for a subhorizontal lid in the roof zone of the complex. Larger augite syenite masses (in parts strongly metasomatized) occur within the agpaitic rocks at the western and northwestern margins of the complex (Fig. 14.1). The field evidence implies that the augite syenite outcrops are relics of a once much larger rock body, which was disaggregated due to the intrusion of agpaitic magma.

Peralkaline granite and quartz syenite occur in several areas of the complex and it is believed that their original extent has been much reduced by erosion (Ferguson 1964; Steenfelt 1981). The largest of these occurrences is in the roof zone of the complex (Fig. 14.1). Alkali feldspar, quartz, sodic amphibole (arfvedsonite) and sodic pyroxene (aegirine) are their major constituents. The perthitic alkali feldspars contain high amounts of tiny aegirine needles, resulting in a green coloration of the rock. Minor components are zircon, astrophyllite, aenigmatite, pyrochlore, sphalerite, fluorite, elpidite, epididymite and others (Ussing 1912; Hamilton 1964; Ferguson 1964). The peralkaline granite and associated quartz syenites post-date the augite syenite but are older than the agpaites. They are regarded as products of an independent silica-oversaturated magma batch (Steenfelt 1981; Stevenson et al. 1997; Marks et al. 2004). The contacts between the different units are not always intrusive but are gradational in places, and it seems possible that assimilation and hybridization may have happened in-situ (Steenfelt 1981). No detailed mineralogical and geochemical study on the peralkaline granites and associated quartz syenites

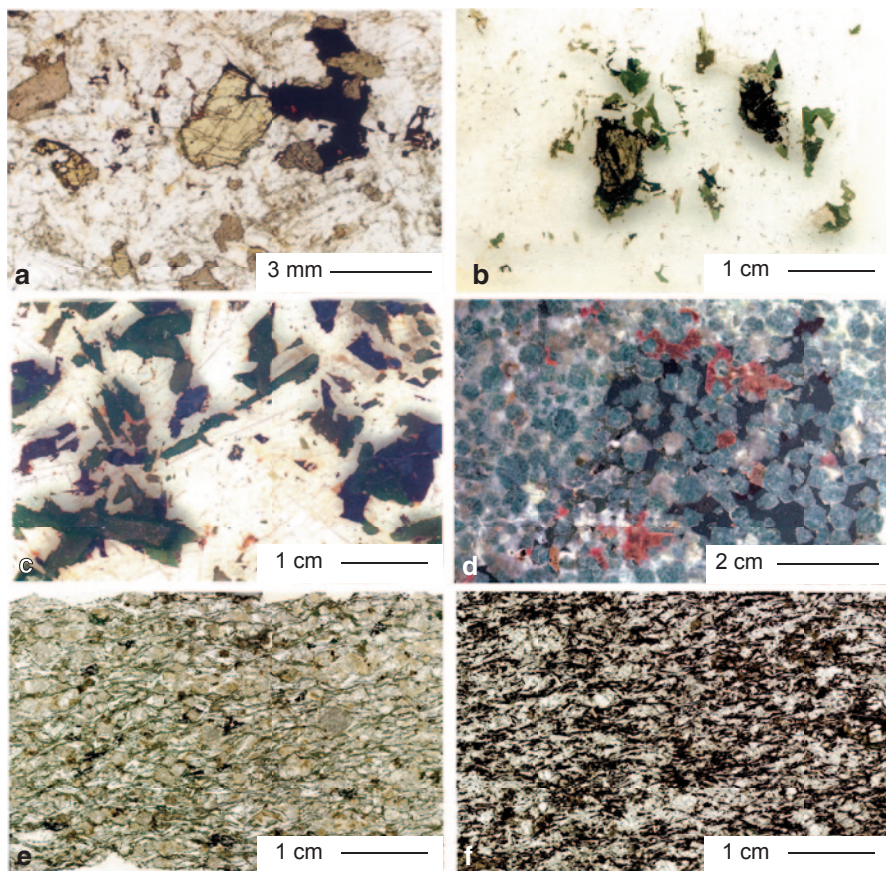


Fig. 14.3 Photographs and microphotographs of the major Ilímaussaq rocks. Note the very different scales. **a** Augite syenite with olivine (*yellow*), augite (*gray*) and ulvöspinel-rich magnetite (*opaque*) in a colorless and cloudy matrix of alkali feldspar with minor amphibole (*reddish brown*). **b** Typical texture in pulaskite with olivine (*yellow*) being replaced by arfvedsonite (*dark bluish*) and aegirine (*green*). **c** Typical foyaite with randomly orientated laths of alkali feldspar and interstitial aegirine, arfvedsonite and aenigmatite. Note the augitic core (*dark gray*) overgrown by green aegirine-rich pyroxene in the lower left corner. **d** Polished surface of naujaite showing euhedral sodalite (*green*) with interstitial arfvedsonite (*black*), eudialyte (*red*) and alkali feldspar/nepheline (*white*). **e** Typical aegirine lujavrite showing needles of aegirine (*green*) and laths of alkali feldspar (*colorless*) wrapping around euhedral phenocrysts of eudialyte and nepheline (*colorless and cloudy*). Note growth of arfvedsonite (*black*) in cases in pressure shadow position of eudialyte. **f** Typical arfvedsonite lujavrite with arfvedsonite (*black*), minor aegirine (*green*) and eudialyte (*round colorless grains*) together with colorless laths of microcline and subhedral nepheline and albite.

is available to date and therefore, the genesis of these rocks, including their genetic relations to the augite syenite and the early agpaite is not well understood.

The peralkaline nepheline syenites represent the main volume of the complex and exhibit large scale stratification: The uppermost nepheline syenites (roof series)

are preserved beneath the augite syenite roof and successively grade from top downwards from pulaskite over foyaite and sodalite foyaite to naujaite, with the latter largely dominating (around 70% of the volume). These rocks are coarse-grained and contain small but appreciable amounts of the same mafic minerals (olivine, augite, magnetite) and apatite as the augite syenite, which are successively replaced by katophorite-arfvedsonite, aegirine-augite to aegirine and aenigmatite (Figs. 14.3b and 14.3c), accompanied by increasing amounts of nepheline and additional eudialyte. Sodalite appears first as an interstitial phase during the foyaite stage but becomes a cumulus phase in sodalite foyaite and naujaite, the latter contain typically around 40–50 vol.% of euhedral sodalite crystals several mm in size (Fig. 14.3d). Interestingly, some of these sodalite crystals occur as hexagonal prisms. They were thought to represent pseudomorphed nepheline (Hamilton 1964), but could also represent paramorphs after a high-pressure polymorph of sodalite (A. Finch, pers. comm.). Besides, fluorite and villiamite occur in significant amounts as several sulfides (e.g., pyrrhotite, sphalerite, galena and djerfisherite) do. The roof series rocks essentially formed by downward solidification in a phonolitic magma. Pulaskite, foyaite and sodalite foyaite represent a border facies, whereas the naujaite formed by the flotation of sodalite less dense than the melt from deeper levels of the magma chamber, followed by compaction and the crystallization of intercumulus melt (Ferguson 1964; Engell 1973; Larsen and Sørensen 1987).

The lowest rocks exposed (floor series) consist of medium- to coarse-grained, mostly layered, apatitic nepheline syenites called kakortokites and are divided into three sub-units (lower layered kakortokites, slightly layered kakortokites and transitional layered kakortokites). The latter grade upwards into typically fine-grained and melanocratic rocks (lujavrites), most of which possess a strong magmatic fabric (Ferguson 1964, 1970; Bohse and Andersen 1981; Andersen et al. 1981, Pfaff et al. 2008; Ratschbacher et al. [submitted](#); Fig. 14.4).

The lower layered kakortokites (LLK) are at least 200 m thick with an unknown continuation at depth. They mainly consist of alkali feldspar, nepheline, arfvedsonite and eudialyte with minor amounts of sodalite, aegirine and aenigmatite together with fluorite, rinkite, pyrrhotite, galena, sphalerite, native Sn and Pb and other accessory minerals. Their layering is defined by the recurrence of on average 8 m thick units (numbered from -11 to +17; Bohse et al. 1971) with pronounced thickness variations between layers (Fig. 14.5a). Most of these 29 units consist of three layers: A basal arfvedsonite-rich layer of black appearance, which is in many cases (but not always) followed by a red eudialyte-rich layer. The upper white layer is rich in alkali feldspar and nepheline and is generally much thicker than the black and red layers (Figs. 14.5b and 14.5c). Within a given three-layer unit, the transitions between the layers are gradual, while the boundaries to consecutive units are often (but not always) sharp (Fig. 14.5b). Generally, the units dip gently (with about 10–20°) towards the center of the intrusion (Fig. 14.5d), with a steepening towards the margin (up to 50°) resulting in a bowl-like geometry (Bohse et al. 1971). One specific unit (+3) contains several hundred meters large inclusions of earlier rock types (augite syenite, naujaite and sodalite foyaite), which were detached from the overlying rocks by a proposed roof collapse (Bohse et al. 1971). The overlying

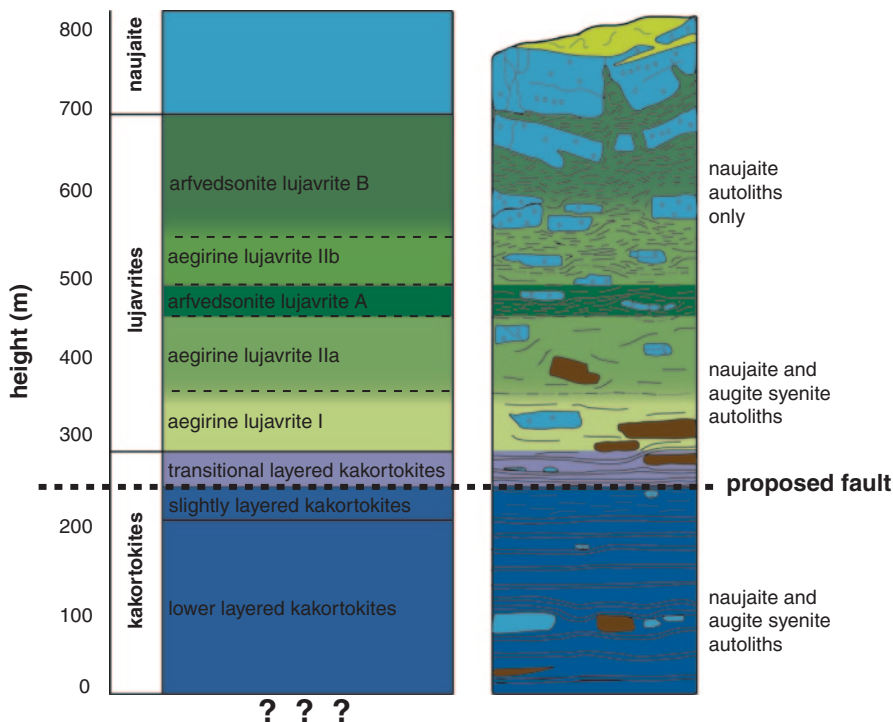


Fig. 14.4 Stratigraphy of the layered kakortokite-lujavrite sequence in the southern part of the complex with major sub-units and the proposed Lakseelv Fault (Modified from Andersen et al. 1981).

kakortokite units envelope these autoliths, and beneath them the layering of the underlying units is depressed (Fig. 14.5e). Other sedimentary structures (i.e. trough banding and current bedding) are mainly confined to the intrusion's margins or occur close to the autoliths (Upton and Pulvertaft 1961; Bohse et al. 1971). An about 50 m thick sequence of finer grained rocks called slightly layered kakortokites (SLK) conformably overlies the LLK (Fig. 14.4). This part of the kakortokites is virtually unlayered and is proposed to have the composition of an average kakortokite (Bohse and Andersen 1981).

A marginal pegmatite zone separates the agpaites from the surrounding augite syenite and country rocks. It forms a rim around the southern part of the complex and is largely restricted to the lower part of the complex made up of kakortokites and lujavrites (Figs. 14.1 and 14.6). The marginal pegmatite zone consists of a mixture of a fine- to medium-grained kakortokite-like matrix cut by a network of pegmatite veins (Fig. 14.8a). The fine- to medium-grained parts of these rocks are considered to represent equivalents of the kakortokite-forming melt (Sørensen 2006). In places, strongly metasomatized autoliths of augite syenite are present in this zone.

On the south shore of the Kangerluarsuk fjord, medium- to fine-grained and melanocratic rocks occur, which were interpreted as representing slumped masses

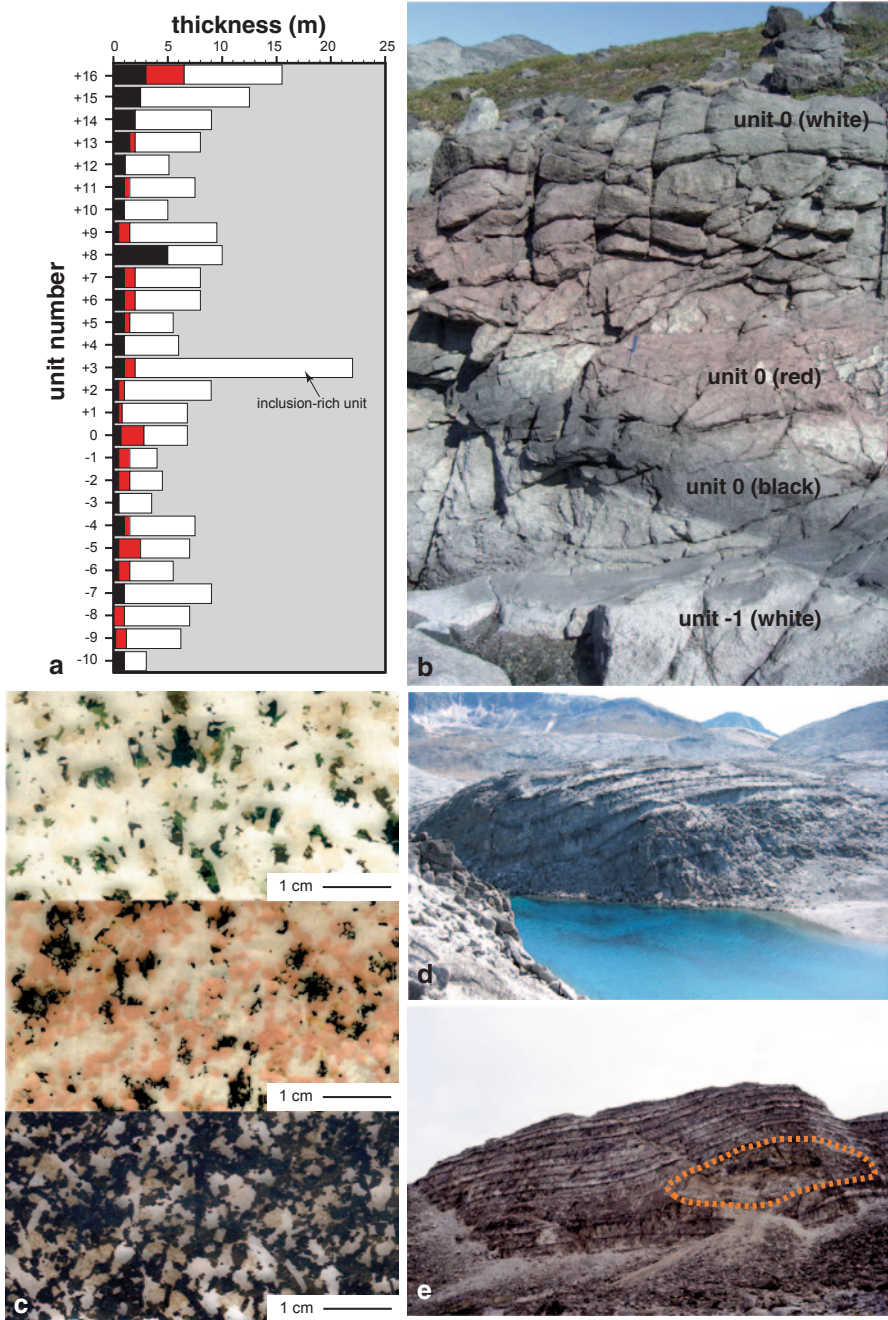


Fig. 14.5 Field appearance of the lower layered kakortokites. **a** Variation of the thickness of black, red and white layers in the different units along the stratigraphy established by Bohse et al. (1971) using their published data. **b** A close-up of unit -1 (white layer) to 0 (black, red and white layer) as exposed in the Laksetværelv valley, the main valley running approximately NW-SE through the LLK sequence (compare Fig. 14.6). Note the sharp contact between the base of unit 0 (black layer) and the

of unconsolidated “kakortokite mush” (Bohse et al. 1971). In places, however, their field appearance and their relationship towards the LLK may also be explained by an intrusive character of these rocks or by mingling (see e.g. Fig. 8 of Bohse et al. 1971). The rocks are mostly arfvedsonite-rich (even compared to the black layers of the LLK) and further contain microcline, albite, aegirine, rinkite, fluorite, sodalite and up to several cm large eudialyte, which often forms clusters in albite-rich schlieren. Their main occurrence is just south of the proposed Lakseelv fault (Fig. 14.6). How important these rocks are volumetrically is unknown and except for their field occurrence, no further work has been published on them. Future work on drill cores throughout the SLK-LLK sequence is required to reveal their significance and to provide data on the hidden rock succession.

Immediately north of the proposed Lakseelv fault, an about 40 m thick sequence of transitional layered kakortokites (TLK) occurs (Fig. 14.6). These show again distinctive modal layering but their dip of foliation is much steeper (45–75° towards NW) than that of the LLK (see above). Unfortunately, the field relations against the other kakortokite units are obscured by alluvial deposits in the Lakseelv valley (Fig. 14.6). Bohse et al. (1971) proposed the presence of a fault in the Lakseelv valley, with a north-down offset that increases from zero at Appat to several hundreds of metres in the Kangerluarsuk Fjord (Figs. 14.1 and 14.6). Based on this, Bohse and Andersen (1981) assigned the TLK sequence to the structurally highest level of the kakortokites in general. The lowest units of the TLK are mineralogically and texturally similar to the LLK, but their grain-size very significantly decreases upwards through the sequence. Furthermore, the modal ratio of aegirine to arfvedsonite increases strongly, continuously developing into the lower parts of the overlying lujavrites.

Lujavrites comprise several varieties of mostly fine-grained and melanocratic apgaitic nepheline syenites, which often show a strong magmatic fabric. A large number of publications deal with the geology, mineralogy and geochemistry of these unusual rocks (e.g., Andersen et al. 1981; Bohse and Andersen 1981; Bailey and Gwodz 1994; Bailey 1995; Rose-Hansen and Sørensen 2002; Sørensen et al. 2003, 2006, 2011; Bailey et al. 1993, 2006; Ratschbacher et al. submitted). Their largest occurrence is in the south-east of the complex to the north and east of the Lakseelv valley (Fig. 14.1). Here the sequence is about 350 m thick and occurs intermediate between kakortokites and naujaite (Figs. 14.4 and 14.6). The lower

top of unit -1 (*white layer*) but the gradual contacts between the black, red and white layers within unit 0. Hammer for scale in the centre of the picture. The viewing direction is approximately towards the east. c Scanned thin sections of a white, red and black unit of the kakortokites. The white one is dominated by alkali feldspar and nepheline with minor amounts of eudialyte (*very pale purple*) interstitial arfvedsonite (*black*) and aegirine (*green*). The red layer is characterized by euhedral eudialyte (*red*) with alkali feldspar, nepheline and interstitial arfvedsonite. In black layers, euhedral to subhedral arfvedsonite dominates with minor amounts of eudialyte (*light brownish*), alkali feldspar laths and nepheline. d Gently dipping layering in the lower layered kakortokites (units +4 to +10) at the SE tip of the Blå Sø, the small lake close to the naujaite autolith as shown in Fig. 14.6. Viewing direction is approximately southwards. e The steep cliffs of Kringlerne as seen from the south shore of the Kangerluarsuk Fjord. The viewing direction is towards the south (compare Figs. 14.1 and 14.6). The cliff is about 110 m high and exposes layers +1 to +13, including unit +3, which contains several larger autoliths of augite syenite, naujaite and foyaite, as marked with the orange dotted line.

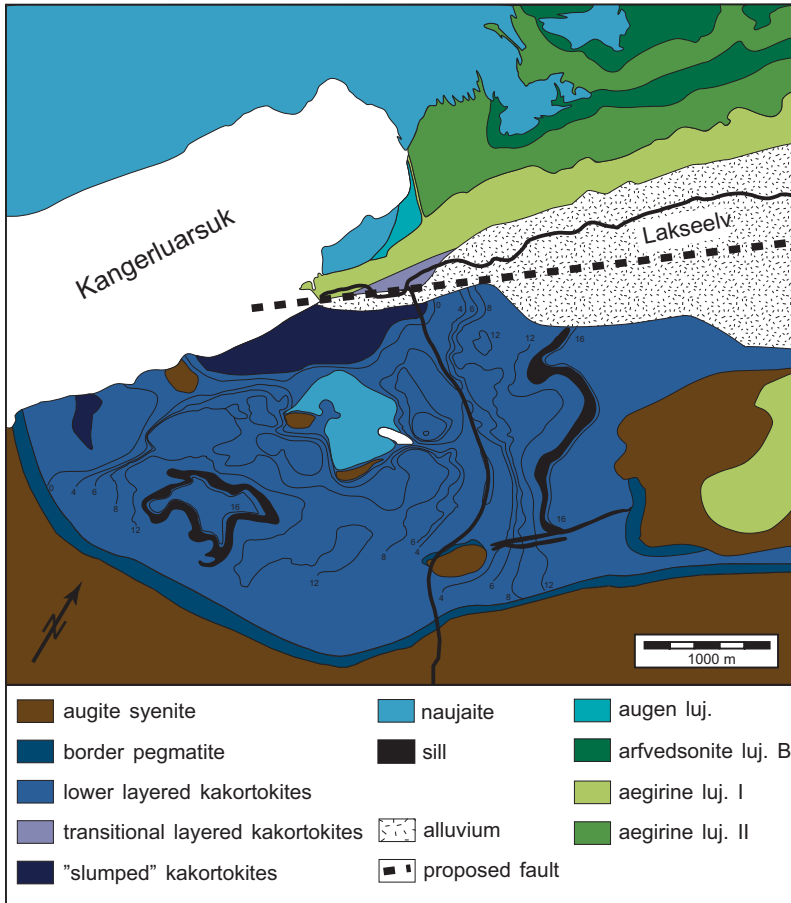


Fig. 14.6 Map of the southwestern part of the Ilmaussaq complex (modified from Bohse et al. 1971 and Andersen et al. 1988). The proposed Lakseelv Fault separates the lower layered kakortokites and the so-called of the complex made up of kakortokites, which grade into the overlying lujavrite sequence. Numbers and thin lines are outcrop traces of black layers of respective lower layered kakortokite units. The lake in the center of the image is the same lake as in Fig. 14.5d The abundant inclusions of naujaite within the lujavrite are omitted for clarity.

part of the sequence gradually evolves from the underlying transitional layered kakortokites (see above) into green aegirine-rich lujavrites (Fig. 14.3e), whereas the upper part is dominated by black arfvedsonite-rich lujavrites (Bohse and Andersen, 1981; Fig. 14.3f). In between, aegirine- and arfvedsonite-dominated sheets of variable thickness alternate. In places these are separated by several dm-thick layers of felsic rocks rich in feldspar and nepheline with smaller amounts of eudialyte, arfvedsonite and aegirine. The lujavrites intrude and disintegrate the naujaites both horizontally and vertically, resulting in a zone where many naujaite blocks of variable size (up to hundreds of meters) occur in a lujavrite matrix, which wraps around them (Fig. 14.7). Mineralogically, lujavrites are similar to the kakortokites

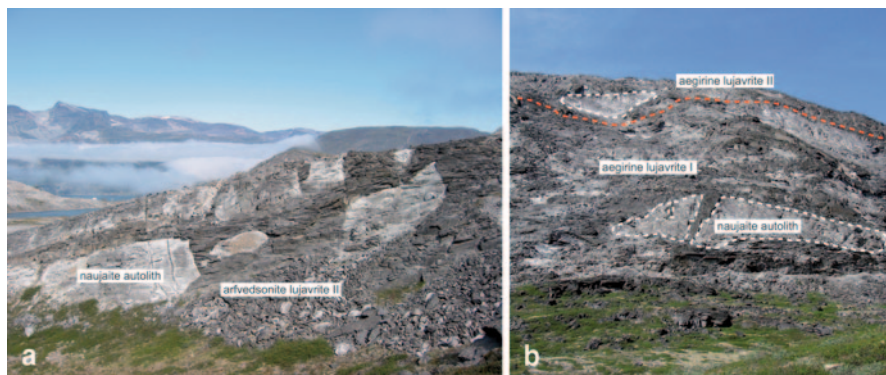


Fig. 14.7 Two photographs of the contact zone between lujavrites and naujaites. **a** Lujavrites intrude and disintegrate the naujaites, resulting in a zone where naujaite blocks are floating within a fine-grained lujavrite matrix. **b** One of the larger naujaite autoliths (about 25 m high), which is split in two parts by intruding aegirine lujavrite I.

except for the high amounts of aegirine in the green lujavrites and the occurrence of microcline and albite instead of perthitic alkali feldspar and abundant interstitial analcime and natrolite in some lujavrites (e.g., Bohse and Andersen 1981). Most of the lujavrites show fluidal textures with a strong alignment of crystals, especially in the aegirine-dominated units (Fig. 14.3e). The initially steep dip (50–85°) towards the NW in the lower part of the sequence first overturns towards SE and within less than 300 m following the Lakseelv valley upwards, the dip rapidly shallows to about 20° towards the NE (Ratschbacher et al. [submitted](#)). Accordingly, the area may be interpreted as a steep feeder zone opening upwards in a fan-like manner. The steeper part is composed of aegirine lujavrite but this flattens out over a short distance whilst grading upwards into arfvedsonite lujavrite B. It is also intersected by approximately horizontal sheets (sills) of arfvedsonite lujavrite A (Ratschbacher et al. [submitted](#)). The field evidence suggests that the lujavrite sequence did not form through continuous closed-system in situ differentiation from a single magma batch but evolved at least partly through melt replenishment from deeper levels.

Further aegirine and arfvedsonite lujavrite occurrences of variable size occur throughout the complex but their detailed genetic relationships to the lujavrites of the Lakseelv area are not known in detail. A number of locally restricted and special lujavrite types are known as well (e.g., M-C lujavrites, augen lujavrite, murmanite lujavrite, villiamite lujavrites and others; e.g., Sørensen et al. 1969; Bohse and Andersen 1981; Figs. 14.1 and 14.6). Some of them may have crystallized from independent magmas whereas others could be products of hybridization and metasomatism with other Ilímaussaq rocks and fluids (e.g., Bohse and Andersen 1981; Sørensen et al. 2011). It is beyond the scope of this review to discuss their genesis in detail.

The lujavrites of the Kvanefjeld area, situated in the northwestern corner of the complex, however, are of special interest (Fig. 14.1). This area represents the roof zone of the complex, where lujavrites are in contact with the volcanic host rocks

(e.g., Sørensen et al. 1969, 1974, 2011; Nielsen and Steenfelt 1979). The geology of this area is exceptionally complex as different Ilímaussaq units, country rocks, gabbros and anorthosites occur as inclusions in a matrix of at least two distinct types of lujavritic rocks, with strong metasomatic overprint and hydrothermal activity (see below). A number of late lamprophyric dyke rocks intersect the area (Sørensen et al. 1969, 2011). The area was recently interpreted to represent an off-shoot from the arfvedsonite lujavrite magma through a fracture zone along parts of the north contact of the complex (Sørensen et al. 2011). One of the latest lujavrite members of this area is rich in naujakasite and steenstrupine. These rocks probably represent some of the final residual melts of the long lasting evolution of the parental magma and are termed hyper-agpaitic rocks (e.g., Khomyakov 1995; Sørensen and Larsen 2001; Andersen and Sørensen 2005). Given their exceptionally high contents of REE, they are of major economic interest.

Kvanefjeld differs from many other emerging REE projects in that it is a multi-commodity project that is also expected to produce U and Zn. Several new target areas in the northern part of the complex (Steenstrupfjeld, Sørensen Zone and Zone 3; Fig. 14.1), each associated with lujavritic rocks, have also been identified as potential economic deposits. To date, these deposits are owned by Greenland Minerals and Energy Ltd (GMEL) and have an estimated resource of 1010 MT containing 593 Milbs U_3O_8 , 11.13 MT RE_2O_3 and 2.3 MTZn (GMEL 2015).

The agpaitic rocks contain abundant pegmatites (Fig. 14.8). They occur as thick layers within a given rock type (e.g., in the naujaite), at the boundaries between different rock types (e.g., the marginal pegmatite; Fig. 14.8a), as discordant dyke-like bodies (Fig. 14.8b) and as irregularly formed lenses enclosed in their host rock (Fig. 14.8c; e.g., Sørensen 1962; Ferguson 1964; Bohse et al. 1971; Müller-Lorch et al. 2007). Throughout the complex, hydrothermal veins containing partly very uncommon mineral assemblages are abundant but are especially concentrated in the Kvanefjeld, on the Taseq slope and some other areas. They show a large range in textures and mineralogical composition (e.g., Engell et al. 1971; Markl 2001a; Markl and Baumgartner 2002; Graser et al. 2008; Hettmann et al. 2014). The most common types include (i) aegirine-dominated veins with variable amounts of albite and analcime (Fig. 14.8d), (ii) albite- analcime- and natrolite-dominated veins, in cases with galena, sphalerite and various Be- and Nb-minerals (e.g., tugtupite, chkalovite, pyrochlore; Fig. 14.8e) and various silico-phosphate and phosphate minerals (e.g., steenstrupine, natrophosphate; Petersen et al. 2001) and (iii) zoned veins with aegirine-rich rims and arfvedsonite-rich cores with or without sodalite, nepheline, albite and analcime (Fig. 14.8f). Furthermore, bitumens are known from some Ilímaussaq rocks (Petersilie and Sørensen 1970; Konnerup-Madsen et al. 1988; Laier and Nytoft 2012). They occur finely dispersed (not visible with the naked eye) in most Ilímaussaq rocks and are also found as millimetre-sized droplets (Konnerup-Madsen et al. 1988). The latter are not well studied to date, but seem especially common in late-stage pegmatites and veins from the Kvanefjeld and Taseq slope rich in Be- and Nb-minerals (H. Friis, per. comm.).

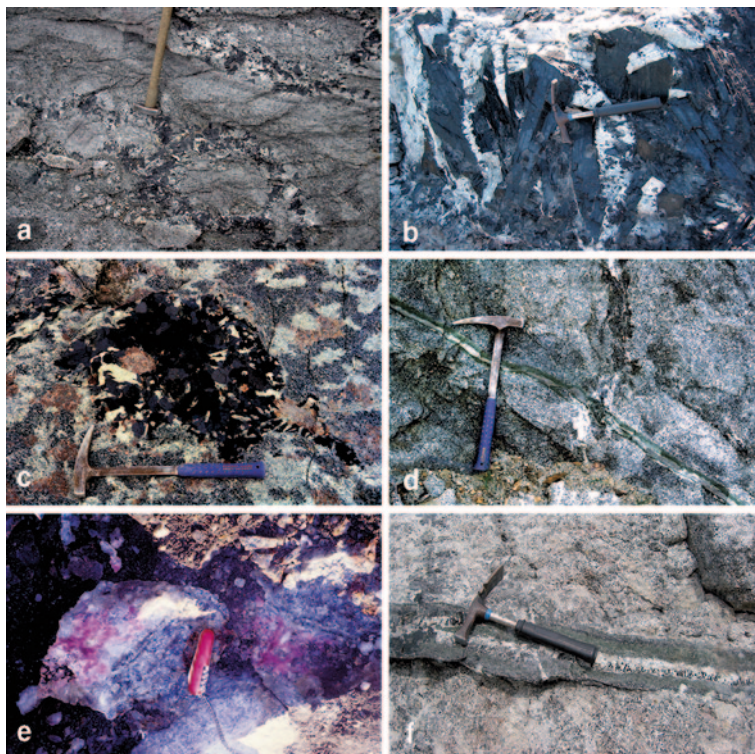


Fig. 14.8 Field photographs of various pegmatites and hydrothermal veins from the Ilímaussaq complex. **a** Close up of the marginal pegmatite area in the southern part of the complex. **b** Discordant arfvedsonite-alkali feldspar pegmatite intruding naujaite. **c** Irregularly formed pegmatite lens enclosed in naujaite. **d** A fine-grained aegirine-albite-analcime vein. **e** Albite- and analcime-rich vein containing purple tugtupite and other Be-silicates like e.g. chkalovite. **f** Zoned vein with a fine-grained aegirine-rich rim and a medium- to coarse-grained core rich in sodalite, nepheline, albite and euhedral arfvedsonite.

A variety of fine-grained sills and dykes occur within the Ilímaussaq complex and its adjacent country rocks (Ferguson 1964; Allaart 1969; Sørensen et al. 1969; Bohse et al. 1971; Rose-Hansen and Sørensen 2001). One of them is an agpaitic and Fe-rich phonolite ($A.I. = 1.44$; $FeO_{tot} = 12$ wt.%) called micro-kakortokite (Fig. 14.1), which was intensively studied (e.g., Larsen and Steenfelt 1974; Marks and Markl 2003; Giehl et al. 2012; 2014). Mineralogically, geochemically and petrologically it shows striking similarities with the various Ilímaussaq rocks and the intruded magma may have had a composition similar to that which produced the agpaitic part of the complex.

Time Constraints

Over the past decades, several attempts to date the Ilímaussaq rocks have been undertaken (e.g., Blaxland et al. 1976; Paslick et al. 1993; Marks et al. 2004; Waight et al. 2002; Krumrei et al. 2006). The results of these studies largely differ in precision but point to the formation of the Ilímaussaq complex at around 1160 Ma. This shows that the Ilímaussaq magmatic system belongs to the youngest of the Gardar intrusive complexes (Upton et al. 2003).

The detailed geochronological study of Krumrei et al. (2006) provides important insights into the duration of intrusion, fractionation and cooling. Baddeleyite from the augite syenite gives an age of 1160 ± 5 Ma, indistinguishable from a U–Pb age of zircon (1166 ± 9 Ma) from the subsequently intruded peralkaline granite (Heaman and Upton, cited in Upton et al. 2003). Amphibole from all major Ilímaussaq rocks (including amphibole from a late-stage pegmatite of the youngest lujavrites) was dated with the Ar–Ar technique and gave a spread in age data which was interpreted to reflect cooling ages (Krumrei et al. 2006). These data and the application of a thermal cooling model led Krumrei et al. (2006) to conclude that the fractionation and cooling history of the complex was very short-lived, probably on the order of 500–800 ka.

Source Constraints and Crustal Contamination

The Ilímaussaq rocks are interpreted to be derived from a parental (transitional) olivine basalt magma that fractionated in a deep-seated magma chamber and was successively tapped by cauldron subsidence and/or stoping (e.g., Larsen and Sørensen 1987; Stevenson et al. 1997). Neodymium and oxygen isotope compositions of mafic minerals from the major rock types are relatively homogeneous ($\epsilon_{\text{Nd}} = -0.9$ to -1.8 and $\delta^{18}\text{O}_{\text{V-SMOW}} = +5.2$ to $+5.7\%$) with no significant difference between the early augite syenite and the agpaites or between early and late agpaites. These data imply that most of the Ilímaussaq melts were derived from an isotopically homogeneous mantle source (Marks et al. 2004). Because of the slightly negative ϵ_{Nd} values, a lithospheric or an OIB-type mantle source is likely but probably accompanied by small amounts of interaction with the host rock during storage in a deeper magma chamber. Trace element data (e.g., enrichment of LILE, LREE, Sr and F) and isotopic signatures of other Gardar dyke rocks and volcanics suggest considerable heterogeneity. It is proposed that these magmas were generated within lithospheric mantle that was variably metasomatized because of earlier subduction processes during the Ketilidian orogeny (e.g., Upton and Emeleus 1987; Halama et al. 2003; Goodenough et al. 2002; Upton et al. 2003; Köhler et al. 2009; Upton 2013). Indeed, potential fragments of the Gardar lithospheric mantle enclosed as xenoliths in an ultramafic lamprophyre were described by Upton (1991) from the small island of Illutalik, just a few of kilometers southwest of the Ilímaussaq complex.

A slightly positive ϵNd value of +0.7 for the above-mentioned micro-kakortokite dyke may imply less contamination with low ϵNd material and thus, this dyke rock may represent the closest approach to the composition of the magma from which the Ilímaussaq rocks crystallized (Marks et al. 2004).

At the margins of the complex, however, crustally contaminated rocks occur (Stevenson et al. 1997) and show that significant assimilation of country rocks occurred on a local scale, probably during emplacement, consistent with field observations of peralkaline granite forming around quartzite xenoliths enclosed in the augite syenite (Ferguson 1964). The peralkaline granite unit has a lower ϵNd (−3.1) and was interpreted to reflect contamination with lower crustal rocks probably at the time of storage (Marks et al. 2004). However, no systematic geochemical investigations on the various occurrences of peralkaline granite and associated quartz syenites are available to date, giving room for further studies. In the following sections, these rocks are therefore not considered further.

Major Mineralogical and Mineral Chemical Changes During the Magmatic to Hydrothermal Evolution of the Ilímaussaq System

Detailed investigations of mineral assemblages and their compositional evolution trends within and between the various rock types provided deep insight in the magmatic evolution of the Ilímaussaq system (e.g., Larsen 1976, 1977b, 1981; Markl et al. 2001; Marks and Markl 2001; Marks et al. 2004; Müller-Lorch et al. 2007; Schmid 2008; Pfaff et al. 2008; Rønsbo 1989, 2008; Zimer et al. submitted; Lindhuber et al. *in press*; Ratschbacher et al. *submitted*). The major results of these studies are briefly summarized below.

From the augite syenite stage to the apgaitic stage the mafic mineral assemblage changes from olivine + augite + Fe–Ti oxides to arfvedsonite (\pm aegirine) + eudialyte + aenigmatite. This is illustrated well by disequilibrium textures found in the apgaitic roof series, where cumulus fayalite, hedenbergite and ulvöspinel are resorbed and replaced by arfvedsonite, aenigmatite and aegirine (Figs. 14.3b and 14.3c). Due to extensive fractionation of olivine and augite, X_{Fe} in mafic minerals increases from intermediate values towards compositions almost devoid of Mg (Fig. 14.9). Besides increasing X_{Fe} , a strong enrichment of Fe_{tot} and depletion of Si in the melts result in increasing Fe/Si ratios. Simultaneously, the relative amount of Na with respect to Ca increases (as mirrored by pyroxene and amphibole evolutionary trends; Fig. 14.9a and b), eventually stabilizing a Na- and Fe-rich mafic mineral assemblage.

In the early apgaites, amphibole generally dominates over pyroxene which, in most cases, is later than amphibole. In most lujavrites, however, primary aegirine and arfvedsonitic amphibole are in textural equilibrium (except for arfvedsonite lujavrite B, where primary aegirine is often replaced by arfvedsonite) and in green

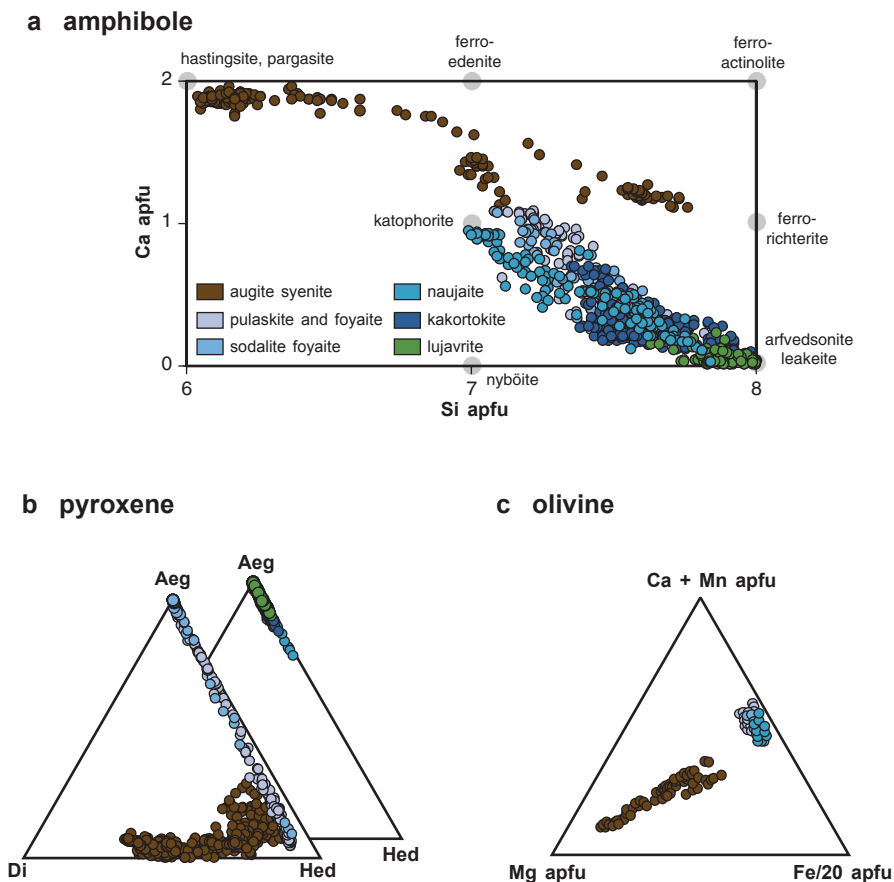


Fig. 14.9 Compositional variation of mafic minerals of the Ilimaussaq rocks: **a** amphibole, **b** pyroxene and **c** olivine (apfu = atoms per formula unit).

lujavrites, aegirine is largely dominating over arfvedsonite (e.g., Rose-Hansen and Sørensen 2002; Ratschbacher et al. [submitted](#)). This was interpreted to reflect changes in water activity and/or redox conditions in the lujavritic melts (e.g., Sørensen 1962; Markl et al. 2001; Rose-Hansen and Sørensen 2002). Slight differences in Na/Si and Na/Fe ratios in the lujavritic melts may also play a role, but the details of the relative stability of aegirine compared to arfvedsonite are to date not quantitatively constrained.

Felsic minerals during the augite syenite stage are alkali feldspar and minor amounts of nepheline, the latter increasing in abundance during differentiation. Ternary feldspar (with up to 20 mol% An) is restricted to the most primitive augite syenite samples from the relatively fine-grained border facies (Larsen 1981; Marks and Markl 2001). In the agpaitic rocks, alkali feldspar, nepheline and sodalite are very abundant and analcime forms during the late-magmatic stage. In some lujav-

vrites, albite and microcline form separate crystals and alkali feldspar is not present anymore.

The formation of large amounts of sodalite (and eudialyte) in the early agpaites clearly reflects the unusual Cl-rich composition of the agpaitic melt and both minerals buffer NaCl activity during differentiation. High levels of F are indicated by the early magmatic occurrence of fluorite and in some agpaitic rocks villiaumite occurs. Because of the high solubility of Ti, Zr and other HFSE in such alkali- and halogen-rich melts (e.g., Watson 1979; Linnen and Keppler 2002), their concentration reaches high values and eudialyte and aenigmatite are stabilized as magmatic phases. These minerals do not occur in the augite syenite, where the HFSE elements are mainly contained in accessory baddeleyite and zircon (Marks and Markl 2001).

Agpaitic pegmatites studied by Müller-Lorch et al. (2007) offer detailed insights into the final stages of agpaitic melt evolution. Mineralogically, they are largely similar to their host rocks. They mainly consist of variable amounts of sodalite, nepheline, microcline, albite and analcime and the dominant mafic mineral is mostly arfvedsonitic amphibole accompanied by aegirine, eudialyte and aenigmatite. Besides others, minor and accessory minerals include fluorite, galena, sphalerite, rinkite, biotite, monazite and in some cases even zircon and various alteration products like natrolite, catapleite, hematite, chlorite, biotite, astrophyllite, aegirine, fluorite and others (Müller-Lorch et al. 2007). However, the generally observed increase of Na/K ratios in early magmatic arfvedsonite is reversed in some analcime-rich pegmatites. These differences are probably related to the buffering of Na and K activities by two coexisting alkali feldspars, which favors Na over K in cooling fluids and the ceasing of the buffer capacity when albite is replaced by analcime as a stable phase (since analcime does not incorporate significant amounts of K). Arfvedsonite in such assemblages is enriched in K (Müller-Lorch et al. 2007). In the very late stages, virtually K-free assemblages in analcime-aegirine veins are present and support the existence of Na-dominated aqueous fluids, augmented by molar Na/K ratios up to about 40 as analyzed by ion chromatography (crush-leach technique) from some late-stage hydrothermal veins (Graser et al. 2008).

Some lujavrites and agpaitic dyke rocks show ocelli-like and spheroidal structures, which have been interpreted as liquid-liquid immiscibility causing the separation of a Na–Al-rich melt from an Fe–Mn–Nb–REE-rich one (Markl 2001b; Sørensen et al. 2003). In some of the latest lujavrites, in fenitized volcanic rocks in the roof of the complex (Kvanefjeld) and in some pegmatites and hydrothermal veins, so-called hyper-agpaitic mineral assemblages formed, which mark an even more evolved stage compared to the agpaites in general (Khomyakov 1995; Sørensen and Larsen 2001; Andersen and Sørensen 2005). The most important mineralogical changes compared to the earlier agpaites include the formation of naujakasite and steenstrupine at the expense of nepheline and eudialyte. They often show complex textural relationships between different mineral assemblages and contain a wealth of otherwise extremely rare and unusual minerals. In these assemblages Na-rich aluminosilicates and phosphates with different amounts of other volatile species (F, Cl and OH) dominate and these rocks recently attracted increased interest as

they contain the highest concentrations of REE. Besides REE, important metals that are extremely enriched during these stages include Be, Nb and Sn, resulting in the formation of various Be-silicates (e.g., tugtupite and chkalovite), Nb-minerals (pyrochlore) and the extremely rare Sn–Be silicate sørensenite. In these final products of the Ilímaussaq evolution several water-soluble minerals like villiaumite, trona, thermonatrite and natrophosphate are stable (Sørensen and Larsen 2001). Recently, even natrosilite was found in some of these rocks (Andersen and Friis *submitted*) as was expected, since it was described from similar assemblages in the Khibina and Lovozero complexes in Russia (Khomyakov 1995; Sørensen and Larsen 2001). Experimental data further imply the co-existence of two immiscible melts during final agpaite evolution: an ionic melt of almost pure NaF and an aluminosilicate melt (Kogarko and Krigman 1970; Kogarko and Romanchev 1983).

Estimation of Crystallization Conditions

Pressure

Based on the observed overburden of the Eriksfjord formation and on fluid inclusion data the emplacement pressure for the Ilímaussaq rocks is around 0.1 GPa corresponding to a depth of about 3–4 km (Konnerup-Madsen and Rose-Hansen 1984). The depth of initial crystallization of sodalite, however, might be significantly deeper, since primary fluid inclusions in sodalite from naujaite imply a pressure of 0.3–0.4 GPa (Markl et al. 2001; Krumrei et al. 2007). This indicates that sodalite crystallized at least partly from a rising magma at considerable depth (around 10–12 km), which requires a conduit towards deeper crustal levels. Based on heatflow data (Sass et al. 1972), however, the agpaite rocks of Ilímaussaq have a total thickness of not much more than 1 km. Sparse gravity measurements indicate that a dense body extending deep into the crust underlies the Ilímaussaq intrusion (Forsberg and Rasmussen 1978) and the aeromagnetic map of the region shows a magnetic low in the Ilímaussaq area (Thorning and Stemp 1997). To date, however, detailed geophysical investigations such as 3-D density modeling (e.g., Arzamastsev et al. 2001) are lacking and thus the deeper structure of the Ilímaussaq area remains open for speculation until such work will be performed.

Temperature and Silica Activity

Overall, the Ilímaussaq rocks cover an extremely long crystallization interval from $>950^{\circ}\text{C}$ to a solidus of around $500\text{--}450^{\circ}\text{C}$ (Larsen 1976; Markl et al. 2001). The highest temperatures were derived by ternary feldspar and nepheline thermometry in augite syenite samples and reach about 1000°C . In the same rocks, near-solidus temperatures deduced from mafic minerals reach temperatures as low as about

650 °C. Silica activity in the augite syenite was initially at about 0.8 and closed system fractionation produced nepheline-bearing assemblages at silica activities of around 0.4 (see Marks and Markl 2001 for details).

Nepheline in sodalite foyaite, naujaite and kakortokites indicates slightly lower temperatures of 950–900 °C and equilibria among nepheline, sodic pyroxene and alkali feldspar indicate temperatures between 800 and 700 °C at silica activities between 0.5 and 0.3. Late-stage aegirine rims around magmatic arfvedsonite indicate temperatures of about 500 °C at silica activities of around 0.25. The highest temperatures in some lujavrites were estimated to 750–800 °C with solidus conditions around 450–500 °C (see Markl et al. 2001 for details) with silica activity dropping from around 0.6 to around 0.15, the latter probably reflecting hydrothermal conditions.

Redox Conditions

During the augite syenite stage redox conditions are constrained by olivine—augite—Fe—Ti oxide assemblages. During fractional crystallization they decrease from about $\Delta\text{FMQ} = -1$ to extreme values around or even below $\Delta\text{FMQ} = -4$, reaching the theoretical stability of native iron (Marks and Markl 2001). These values represent some of the most reduced conditions reported for terrestrial plutonic rocks. Similar redox conditions ($\Delta\text{FMQ} = -2$ to -4) were derived from preserved relics of the same assemblage in pulaskite and sodalite foyaite, which shows that the initial stages of agpaite formation were similarly reduced (Schmid 2008). These estimates are in agreement with the presence of ulvöspinel-rich magnetite as well as with experimental evidence (Giehl et al. 2012).

The quantification of redox conditions during the main agpaite stage is difficult due to the absence of suitable mineral assemblages for which reliable thermodynamic data exist. Nevertheless, the presence of primary methane-dominated and water-free fluid inclusions, as found in most agpaites (e.g., Krumrei et al. 2007), and low sulfate/sulphide ratios found in sodalite from naujaites, again indicate relatively reduced conditions (Hettmann et al. 2012). The high amount of Fe^{3+} in clinopyroxene of the agpaite rocks does not contradict these observations, since the $\text{Fe}^{2+}/\text{Fe}^{3+}$ ratio in silicate melts depends not only on oxygen fugacity, but is largely influenced by peralkalinity, the presence of water and other factors (Botcharnikov et al. 2005; Giuli et al. 2012; Markl et al. 2010).

During late-magmatic to hydrothermal stages, relatively oxidized conditions (around and above the HM buffer) were estimated for the formation of some skarn-like rocks as well as for some hydrothermal veins (Graser and Markl 2008; Karup-Møller 1978). Similar evolution trends starting with highly reduced conditions at magmatic stages evolving towards relatively oxidized during hydrothermal stages are known from other peralkaline rock suites and seem to be a typical feature of peralkaline magmatic systems (e.g., Marks et al. 2003; Mann et al. 2006; Markl et al. 2010).

Fluid Evolution

Numerous studies investigated the nature and composition of fluids trapped in minerals of the Ilímaussaq complex, mostly focusing on the agpaite rocks and their associated hydrothermal veins (e.g., Sobolev et al. 1970; Petersilie and Sørensen 1970; Konnerup-Madsen 1980, 1984, 2001; Konnerup-Madsen and Rose-Hansen 1982, 1984; Konnerup-Madsen et al. 1979, 1981, 1985, 1988; Markl and Baumgartner 2002; Krumrei et al. 2007; Graser et al. 2008). These studies revealed the complex fluid evolution in Ilímaussaq and the unusual fluid composition: Fluid inclusions in the Ilímaussaq rocks are dominated by hydrocarbon gases (mostly methane) and hydrogen.

Presumably primary fluid inclusions in early magmatic sodalite from the roof and early magmatic sodalite and eudialyte in the floor cumulates are predominantly either methane-dominated (with minor amounts of hydrogen) or pure methane with generally no detectable water (not even with Raman techniques; Konnerup-Madsen et al. 1985; Krumrei et al. 2007). This was interpreted to result from strongly reduced conditions and low water activities during the early stages of agpaite crystallization and is in accordance with mineralogical observations and petrologic calculations (see above). Fluid inclusions of secondary origin in the same rocks are either methane-dominated (containing traces of higher hydrocarbons like ethane and propane) or aqueous, with high salinities of up to about 22 wt.% NaCl equiv. (e.g., Konnerup-Madsen et al. 1988; Markl et al. 2001; Krumrei et al. 2007). Krumrei et al. (2007) presented a two-stage model for the evolution of the Ilímaussaq fluid phases due to the much higher solubilities of water than hydrocarbons in silicate melts. At the beginning of sodalite crystallization, a hydrocarbon-rich fluid was in equilibrium with the agpaite melt. The water activity in the agpaite melt at this stage was very low (Markl et al. 2001). NaCl activity in the melt decreased with further sodalite fractionation from initial values of about 0.4 down to values well below 0.1, while the water activity successively increased. During late-magmatic conditions, analcime became stabilized instead of albite and nepheline (Ussing 1912; Markl et al. 2001; Müller-Lorch et al. 2007) and eventually, an aqueous fluid was expelled from the melt. Because NaCl strongly partitions into the aqueous fluid, the large-scale formation of sodalite ended with the exsolution of this aqueous fluid, which was then trapped only as secondary inclusions. In lujavrites, however, two types of apparently primary fluid inclusions occur: firstly again methane-dominated ones and secondly aqueous fluid inclusions with relatively low salinities (around 3 wt.% NaCl equivalent; Markl et al. 2001), pointing to the entrapment of two co-existing and immiscible water-rich and methane-rich fluid types (Konnerup-Madsen 2001).

Primary and secondary fluid inclusions in late-magmatic to hydrothermal veins are highly variable ranging from again hydrocarbon-dominated via hydrocarbon–water–NaCl mixtures to aqueous fluid inclusions with highly variable salinities with or without traces of hydrocarbons (e.g., Konnerup-Madsen and Rose-Hansen 1982; Graser et al. 2008). Detailed investigation on some of the late-stage agpaites and associated hydrothermally overprinted rocks revealed a large temperature range (from about 600–200 °C) for their formation, which marks the transition from the late-magmatic to the hydrothermal, now hyper-agpaite stage (see above; Markl

2001a; Sørensen and Larsen 2001). The aqueous agpaite fluids are characterized by a high pH (up to 10–12) enabling the formation of ussingite and the above-described hyper-agpaite mineral assemblages (Markl and Baumgartner 2002). Kogarko (1977) and Khomyakov (1995) proposed a gradual transition from melt to hydrothermal fluid in such systems. Indeed, today it seems clear that the Ilímaussaq rocks are an exceptional archive for such a transition and the detailed study of these final products of agpaite evolution may reveal further details of this process, which to date is only fragmentally understood.

Methane-rich fluid inclusions with minor amounts of hydrogen and higher hydrocarbons and the occurrence of bitumen are also known from other agpaite complexes (especially from the Kola peninsula) and may be a general characteristic of such rocks (e.g., Nivin 2002). Despite many studies, there was and is considerable debate whether such fluids are of a magmatic origin and represent primary high-temperature conditions (mantle gas theory) or are the result of various secondary processes (e.g., Konnerup-Madsen 2001; Potter and Konnerup-Madsen 2003; Krumrei et al. 2007; Graser et al. 2008; Beeskow et al. 2006; Nivin et al. 1995, 2001, 2005; Potter et al. 1998, 2004; Potter and Longstaffe 2007), but scientists agreed on the abiogenic origin of the methane-rich fluids found in the Ilímaussaq rocks and in similar agpaite complexes in Russia (see above). This was, however, largely questioned by Laier and Nytoft (2012) who argued that the hydrocarbons of Ilímaussaq are of biogenic origin and migrated to Ilímaussaq from deep oil seeps offshore west of Greenland during the Cretaceous. Laier and Nytoft (2012) investigated the biomarker distribution in finely dispersed bitumens in the Ilímaussaq rocks. They concluded that a biogenic origin would be consistent with published stable isotope data for the bitumen, and even re-interpreted the published stable isotope characteristics of hydrocarbon gases from Ilímaussaq and from the agpaite Khibina and Lovozero complexes in Russia mostly as of biogenic origin. Loss of hydrocarbon gases via diffusion (as reported from Khibina and Lovozero by Nivin et al. 2001, 2005) may significantly change their isotopic composition (Zhang and Kross 2001) and this process is invoked by Laier and Nytoft (2012) to be the reason that hydrocarbon gases from Ilímaussaq, Khibina and Lovozero could be mistaken as abiogenic gases. This theory is in stark contrast to numerous detailed fluid inclusions studies (see above) and has to be regarded as dubious until it can be documented that such fluids have also been trapped in minerals outside the Ilímaussaq complex as one would expect, if they migrated from deep oil seeps offshore west of Greenland. Hydrocarbons in the Ilímaussaq rocks are in agreement with the predicted behavior of the C–O–H system under the extremely reduced crystallization conditions reported for the Ilímaussaq magmas (e.g., Holloway and Jakobsson 1986; Scott 2004; Zhang and Duan 2010; Mysen and Yamashita 2010). So far the idea of Laier and Nytoft (2012) has to be regarded as highly unlikely and it is the responsibility of Laier, Nytoft and their followers to present the supporting evidence that the application of biomarker distributions to such magmatic to hydrothermal rocks is a reliable source of information. Obviously, the source and origin of the hydrocarbons and especially that of the so-far little studied bitumen in Ilímaussaq (and other agpaite complexes) is an exciting topic which needs further investigation.

Metasomatic and Hydrothermal Processes

The fluids associated with the Ilímaussaq magmas caused intense metasomatism and hydrothermal overprint within the complex, at its margins, and in the surrounding country rocks, resulting in highly variable secondary mineral assemblages (e.g., Ferguson 1964; Sørensen et al. 1969; Graser and Markl 2008; Derrey 2012). Furthermore many varied types of hydrothermal veins (see above) and several hundreds of square meters large albitized and analcimized areas as well as oxidized and hematitized zones throughout the complex demonstrate the role of intensive late-stage fluid circulation both pervasive and channelized (e.g., Ferguson 1964; Engell et al. 1971).

In most rock types, the primary mineral assemblages are resorbed and replaced by secondary minerals to variable extents (see above): The olivine-augite-ulvöspinel assemblage is replaced by katophorite-arfvedsonite, aenigmatite and aegirine-augite (Fig. 14.3, e.g., Larsen 1976; Markl et al. 2001); primary apatite (up to 21 wt.% REE₂O₃) became unstable, was dissolved and recrystallized to several new generations of apatite with partly high Na- and REE contents (up to 2.9 and 27 wt.%, respectively; Rønsbo, 1989, 2008; Zirner et al. submitted) and felsic minerals (alkali feldspar, sodalite and nepheline) are commonly replaced by pure albite, analcime, secondary sodalite, nepheline, natrolite and other zeolithes (e.g., Ferguson 1964; Markl et al. 2001). Eudialyte is often altered to complex mixtures of albite, aegirine, microcline, catapleite, fluorite, monazite, apatite, neptunite, rarely zircon and a wealth of other REE-rich minerals (e.g., Rose-Hansen and Sørensen 2002; Karup-Møller et al. 2010; Karup-Møller and Rose-Hansen 2013). Furthermore, autoliths of various Ilímaussaq rocks within younger members of the complex are overprinted to variable degrees causing similar mineralogical changes (e.g. Schönenberger et al. 2006).

Although there exists a large variety of different kinds of hydrothermal veins in the complex, only the Be silicate-bearing ones were investigated in greater detail (Engell et al. 1971; Markl 2001a; Markl and Baumgartner 2002). Their field relations imply that they (at least partly) replaced earlier Ilímaussaq rocks and their microtextures and mineral assemblages point to strongly basic pH values for the responsible fluids (or melts?) governing the formation of minerals like ussingite and tugtupite (Markl and Baumgartner 2002) during hyper-apatitic conditions (see above).

At the margins of the complex, Ca-rich skarn-like rocks with ilvaite-grossular-, and epidote-bearing assemblages occur. Their formation was interpreted in a model in which seawater was the metasomatizing fluid which entered the surrounding basaltic lavas, reacted with them (spilitization) and infiltrated Ca along fractures into the metasomatized rocks (Graser and Markl 2008). Further evidence for the infiltration of seawater along the margins of the complex is provided by Li and B isotope studies of Marks et al. (2007) and Kaliwoda et al. (2011).

Metasomatism in the country rocks of the complex was first described by Ferguson (1964). Detailed work of Derrey (2012) showed that in the granitic country rocks along the South coast of the Kangerluarsuk fjord metasomatism occurred up to at least 120 m away from the contact. Several effects on the granitic country rocks

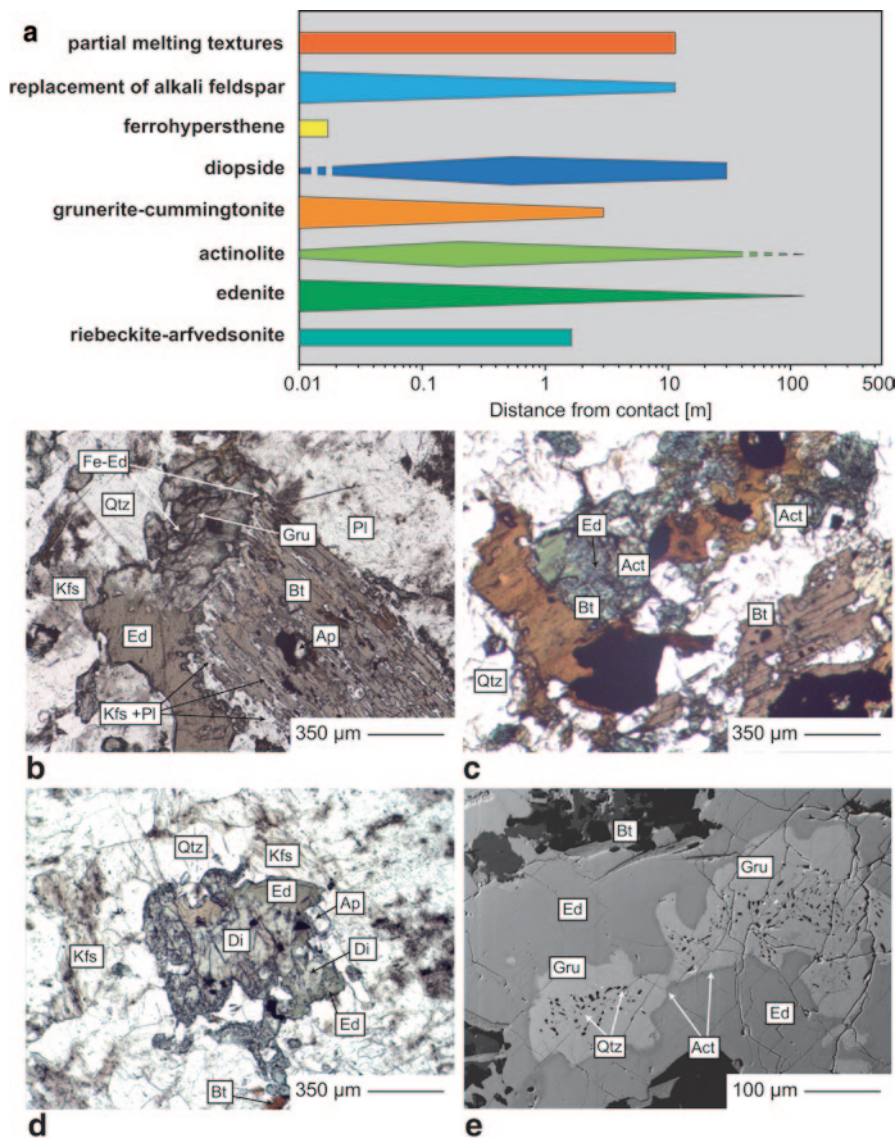


Fig. 14.10 Mineralogical and textural effects on the granitic country rocks caused by the emplacement of the Ilimaussaq complex (modified from Derrey 2012). **a** Overview on the textures and minerals found in the country rock against distance from the contact. **b** Breakdown of biotite with newly formed grunerite that is overgrown by edenite. **c** Intergrowth of actinolite and edenite replacing biotite. **d** A diopside core mantled by edenite. **e** BSE image of grunerite with tiny quartz inclusions, rimmed by a thin actinolite seam, which is overgrown by edenite.

caused by the emplacement of the Ilimaussaq complex can be distinguished and a detailed textural analysis allows the assessment of their relative timing (Fig. 14.10). First of all, the granite was heated to about 670 °C causing partial melting of the granite as recorded by granophyric intergrowth textures of alkali feldspar and quartz up

to about 10 m away from the contact. This heating triggered several dehydration reactions of primary biotite, which led to the formation of pyroxene (ferrohypersthene and diopside) and amphibole (grunerite-cummingtonite series compositions). The granite was further overprinted by pervasive infiltration of fluids with variable Ca/Na ratios causing (i) the formation of two generations of calcic amphibole (actinolite and edenite), which overgrew the above-mentioned biotite-breakdown products and (ii) the replacement of alkali feldspar by plagioclase and quartz. Subsequently, sodic amphibole (riebeckite-arfvedsonite series compositions) formed in samples very close to the contact and lastly, the occurrence of aegirine-rich veins (in cases with eudialyte) indicate channelized infiltration of late agpaitic fluids into the granitic country rocks (Derrey 2012).

In all, the products of intensive late-stage fluid-assisted processes within and around the Ilímaussaq complex are plentiful and variable. These aspects of the Ilímaussaq evolution need to be investigated in detail, in order to better understand the physical and chemical characteristics of agpaitic fluids and their capability for transporting and concentrating HFSE and other unusual elements (e.g., Be, Sn) to sub-economic or economic interest. Clarifying the potential role of hydrocarbons and bitumen in such systems is another important task to achieve.

Combining Detailed Mineral Chemical and Structural Data: New Insight Into the Formation of the Layered Kakortokite-Lujavrite Sequence

Igneous layering has been described in almost all of the major Gardar plutonic complexes and from some of the larger dykes, covering a remarkably wide compositional spectrum of rocks (see Upton et al. 1996 for a review). In the Ilímaussaq complex itself, different forms of igneous layering are present in all rock types (e.g., Sørensen and Larsen (1987), but have been mostly studied in the kakortokites. Since their first description by Ussing (1912) their origin has been widely discussed, resulting in a number of very different models for their formation. These include intermittent crystallization of a multiply saturated magma (Ussing 1912; Sørensen, 1968), convective overturns (Upton and Pulvertaft 1961; Bohse et al. 1971), crystallization from a multiply layered magma chamber (Larsen and Sørensen 1987; Bailey 1995; Bailey et al. 2006), recurrent magma recharge (Pfaff et al. 2008) and changes in vapor pressure (Ussing 1912; Pfaff et al. 2008). A satisfactory model for the layering observed in the kakortokite sequence needs to explain at least the following features:

1. The formation of three-layer units with internal mineral grading, but with sharp upper and lower contacts between units of the lower layered kakortokites and the absence of clear layering in the overlying slightly layered kakortokites.
2. The recurrence of these rhythmic units of at least 29 times and their relative continuity over several kilometers.

Furthermore, the transitional layered kakortokites evolve gradually (structurally and mineralogically) into the lujavrite sequence. Their genetic relationship towards slightly layered kakortokites and lower layered kakortokites, however, are unclear (see above).

The Formation of Three-Layer Units

Textural evidence implies that amphibole, eudialyte, and alkali feldspar + nepheline crystallized more or less contemporaneously (e.g., Sørensen 1968; Pfaff et al. 2008; Lindhuber et al. *in press*), hence there must have been an effective mechanism which separated these minerals from each other after crystallization. Given the significant density contrast between these phases ($\rho_{\text{arfvedsonite}} > \rho_{\text{eudialyte}} > \rho_{\text{alkali feldspar}} \sim \rho_{\text{nepheline}}$), the modal grading within a given unit is believed to be due to gravity settling (e.g., Sørensen 1968; Larsen and Sørensen 1987; Pfaff et al. 2008). Field observations support this assumption: Arfvedsonite is strongly concentrated at the base of each unit (black layer), eudialyte is enriched in the middle (red layer) while upper white layer is rich in the light minerals (alkali feldspar + nepheline), with gradual transitions between the three layers of a given unit (Fig. 14.5b). This process is convenient to explain the formation of the modally graded three layer-units.

The overlying slightly layered kakortokites do not show clear modal layering and are finer grained than the lower layered kakortokites. Obviously, gravitational sorting processes were not effectively working in this upper sequence and these rocks may therefore represent an “upper border facies” of the kakortokites, similar to the pulaskite-foyaite-sodalite foyaite succession for the roof series rocks. However, detailed studies on the slightly layered kakortokites are needed in order to clarify their origin and to integrate these rocks into a comprehensive model.

Crystal Mat Formation and the Origin of the Layered Kakortokite Sequence

The recurrence of the three layer-units for at least 29 times (this is the number of three-layer units exposed today, with an unknown continuation at depth), however, is much less clear and cannot be explained by gravitational sorting of sinking minerals in a melt alone. An overview study on the compositional changes in eudialyte from black layers throughout the kakortokite sequence revealed surprisingly small indication of fractional crystallization upwards through the lower layered kakortokite sequence with only slightly decreasing Fe/Mn ratios in eudialyte (Fig. 14.11; Pfaff et al. 2008). A recent study by Lindhuber et al. (*in press*) focused on two sampling sites within the kakortokite sequence covering one and two three-layer units, respectively, including samples from the overlying base (black layer) of the next unit as well as from the top (white layer) of the underlying unit (Fig. 14.12). At

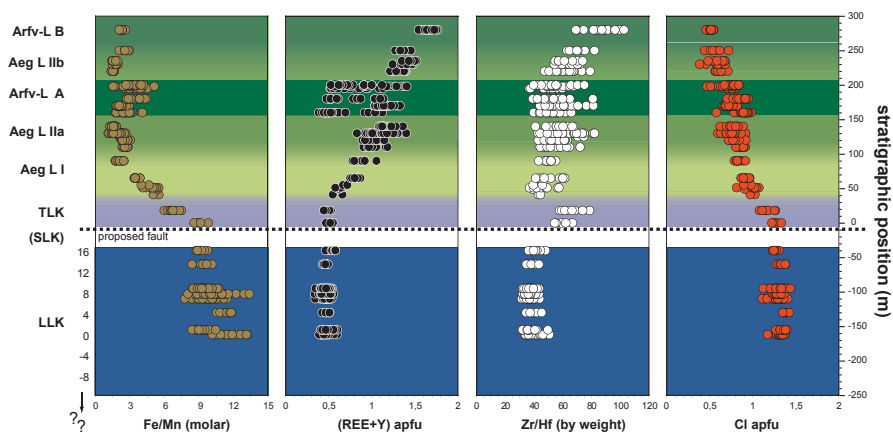


Fig. 14.11 Variation of eudialyte composition throughout the kakortokite-lujavrite sequence (Data from Pfaff et al. 2008; Lindhuber et al. *in press* and Ratschbacher et al. *submitted*). In lower layered kakortokites (LLK) only data for black layers are shown, for slightly layered kakortokites (SLK), no such data exist to date.

both sampling sites, the Fe/Mn ratio of eudialyte continuously decreases from the base (black layer) towards the top (white layer) of a given unit, which is interpreted to reflect fractional crystallization within a three layer-unit. The base of the overlying units (black layer), however, starts with a slightly higher Fe/Mn ratio (and thus less evolved), generally decreasing upwards through the sequence, resulting in a “christmas-tree pattern”. This is indication for relatively little but detectable fractional crystallization within the lower layered kakortokites sequence. The black layer of unit seven, however, is less evolved than that of the underlying unit six (Fig. 14.12). This reset of the Fe/Mn ratio is associated with a small-scale fold at the contact between units + 6 and + 7, which may indicate post-cumulus movement within a semi-rigid crystal mush.

The model of mat formation and crystal settling in a magma chamber as introduced by Lauder (1964) and later invoked for the Skaergaard intrusion by Nielsen and Bernstein (2009) and Namur et al. (2015) can explain the recurrence of the kakortokite layering and is consistent with the observed changes in eudialyte composition. In a non-convecting magma chamber (as was proposed for the kakortokites by Sørensen (1968) and Sørensen and Larsen (1987)), cumulate minerals nucleate and grow throughout the magma. The heavier minerals (amphibole and eudialyte) would sink, while light minerals (alkali feldspar) would start to float. One possibility to produce a melt dense enough for feldspar to float is to crystallize large amounts of light minerals (sodalite) during an early stage. As cooling of the magma continues, amphibole, eudialyte and feldspar start to crystallize and the sinking amphibole and eudialyte interfere with the buoyant feldspar causing “traffic jams” (Bons et al. 2015). These crowding effects may result in amphibole-rich mats underlain by alkali feldspar-rich horizons (the later black and white layers). With time, the amphibole mats would further grow by the addition of more sinking amphibole crystals,

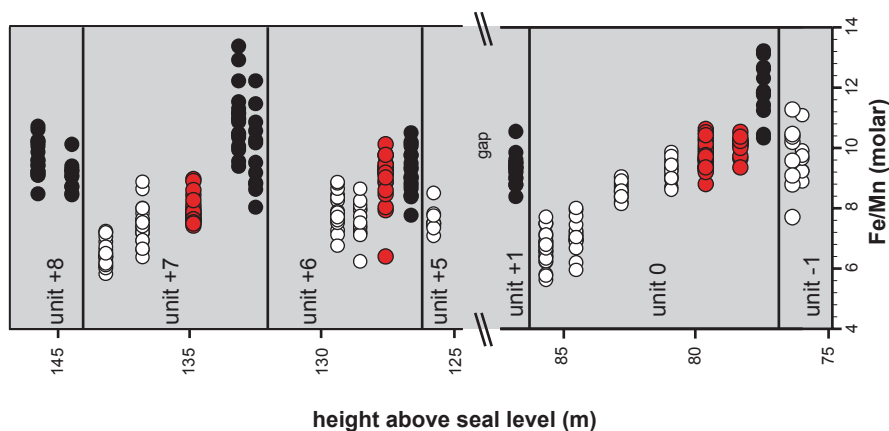


Fig. 14.12 Compositional variation of eudialyte in eudialyte from units -1 to $+1$ and $+5$ to $+8$, color-coded for *black*, *red* and *white* layers for the respective units (Data from Lindhuber et al. *in press*).

by intercumulus growth of grains already contained in the mat and by crystallization of melt pockets within the crystal mats. Hence, effective barriers would build up over time and the remaining melt and crystals between two of such amphibole barriers would eventually evolve as quasi-closed systems (Fig. 14.12). In such a scenario, the lowest mat within a given magma column would contain the earliest crystallized eudialyte with relatively high Fe/Mn ratios, because early crystallized eudialyte crystals may have been dragged down by amphibole and hence enclosed in the amphibole-mats before they became impermeable—consistent with the data of Pfaff et al. (2008) and Lindhuber et al. (*in press*). Relatively similar Fe/Mn ratios in eudialyte from black layers in the upper part of the lower layered kakortokites sequence (Pfaff et al. 2008) may imply that these were trapped in the amphibole-rich mats and were thereby protected from further equilibration with the evolving liquid and from exchange over unit boundaries. Thus, relatively primitive eudialyte grains should be present within all black layers, independent of their stratigraphic height. Later eudialyte crystallized from the evolving melt between two amphibole mats should then show decreasing Fe/Mn ratios upwards the sequence with distinct resets of the ratios between different units—again, consistent with the data of Lindhuber et al. (*in press*).

In all, the structural and mineral chemical features of the lower layered kakortokites can be explained by the proposed mechanism of mat formation associated with crowding effects. With time, amphibole-rich mats would sink downwards and a partly consolidated (and layered) kakortokite mush would accumulate from below. The presence of autoliths of other Ilimaussaq rocks within a distinct horizon of the lower layered kakortokites shows that such quasi-solid floors existed, whilst further upwards such mats were still forming.

A quantitative treatment of crowding effects and mat-forming processes in the lower layered kakortokites is given by Baur (2012) and Bons et al. (2015) and fur-

ther implies that (depending on melt viscosity and a number of other factors) the formation of a thick layer of low-density minerals (e.g., sodalite) above a rhythmically layered sequence is also possible. This raises the possibility that parts of the naujaite may have formed simultaneously to kakortokites (see Sect. “Geological Setting”). Indeed, cryptic layering in the naujaite is evident from trace elements (Br, I, B, S) in sodalite and at least two naujaite units can be distinguished (Krumrei et al. 2007; Bailey 2006). Also, detailed work is currently in progress in order to test if the mat formation model could also produce the chemical trends which apparently imply a refilling of the system with a less evolved magma (see above) that contradict the field observations so far.

Surprisingly, the review by Naslund and McBirney (1996) on mechanisms of formation of igneous layering does not include the mat formation process proposed by Lauder (1964), although potentially representing a valid explanation for the formation of rhythmic layering in general. Recently, however, this process was invoked to explain layering features observed in the Triple Group of the Skaergaard intrusion (Nielsen and Bernstein 2009; Namur et al. 2015) and it remains to be tested if the process of mat formation during crystal settling can explain the recurrence of rhythmic layering in other multiply saturated (anchieutectic) layered intrusions as well.

The Magmatic Evolution and Architecture of the Lujavrite Sill Complex

Pfaff et al. (2008) and Ratschbacher et al. (submitted) performed detailed studies on the compositional variation of eudialyte (which is a component of the early cumulus assemblage) throughout the transitional layered kakortokite-lujavrite sequence (Fig. 14.11). An almost continuous trend with strongly decreasing Fe/Mn and increasing (REE + Y) throughout the sequence is believed to reflect fractional crystallization (Pfaff et al. 2008; Ratschbacher et al. submitted). The simultaneous decrease of Cl in eudialyte may reflect an increase of water activity during lujavrite evolution, consistent with petrological calculations and fluid inclusion data (see above). In arfvedsonite lujavrite A, however, a reset to less evolved melt compositions (lower REE + Y and higher Fe/Mn in eudialyte) may have resulted from an influx of less evolved melt into the lujavritic magma bodies (Ratschbacher et al. submitted). This is consistent with observations of intrusive contacts between aegirine lujavrite IIa and arfvedsonite lujavrite A and suggests that the latter is a separate sheet intruded into aegirine lujavrite IIa instead of being an in situ differentiate from it.

Ratschbacher et al. (submitted) presents mineral chemical evidence indicating that at least two melt batches were responsible for the formation of the lujavrite sequence in the Lakseelv area, challenging the classical view of a continuous closed system evolution for the lujavrites (Sørensen 2006). The lujavrite sequence including the TLK is probably a distinct unit of the Ilímaussaq complex and may represent

the remnants of a steep feeder zone once forming a sill complex consisting of at least two magma batches (see Sect. “Field Relations among Major Rock Types and General Structure of the Complex”). They intruded the naujaites both horizontally and vertically (Fig. 14.7). The texturally and structurally distinct M-C lujavrites west of Appat (Fig. 14.1) are probably products of another independent magma body.

A direct genetic relationship between lujavrites of the Lakseelv area and the LLK is questionable as is the significance of the spatially associated “slumped kakortokites” (Bohse et al. 1971). We speculate that the Lakseelv valley may be the trace of a shallow northwards dipping flexure or fault, which juxtaposed the layered kakortokites of Kringlerne against their once overlying naujaites. This triggered and channeled the intrusion of a feeder system for lujavrite-forming melts. Based on preliminary structural data on the lujavrite sequence, including foliations, lineations and shear-sense indicators, such movements were active during super-solidus and sub-solidus conditions of the lujavrites (Ratschbacher et al. [submitted](#)). However, detailed structural follow-up work, including the interpretation of microstructures in the lujavrites and in the “lujavrite-naujaite inclusion zone” are needed to clarify such important structural details. Other modern methods like AMS measurements (e.g., O’Driscoll et al. 2006) are promising tools to answer such questions about the architecture of plutonic systems. Also, detailed structural investigations in the closer and broader vicinity of the complex could probably improve the still sketchy picture of the tectonic evolution of the Gardar rift system and may help to understand how the emplacement of the Ilímaussaq magmas was influenced by tectonic structures (e.g., Ussing 1912; Ferguson 1964).

What is the parental magma of the Ilímaussaq complex?

The present model for the petrogenesis of the Ilímaussaq complex involves a deep-seated magma chamber, which was successively tapped resulting in several magma batches showing variable degrees of differentiation. These were successively emplaced at a shallow crustal level (e.g., Sørensen and Larsen 1987). Tracking and reconstructing the detailed geochemical evolution of the Ilímaussaq melt(s) is complicated by the fact that most rock types are the result of crystal fractionation and cumulate formation, and there is appreciable ambiguity about the detailed genetic relations between the different rock types and the number of magma batches involved in the formation of the complex (see above). Thus, when searching for a potential parental melt composition of the Ilímaussaq magmatic system, the first question must be: parental to which stage of the evolution? Parental to the augite syenite stage, the apgaitic stage, or parental to the whole complex?

New Experimental Evidence for the Augite Syenite—Agpaitic Relations

There has been considerable debate about the detailed genetic relationships between the augite syenite and the early agpaites (e.g., Engell 1973; Sørensen 1978; Bailey et al. 1981). To date, it is not entirely clear if agpaites evolved continuously from augite syenites via fractional crystallization at depth or if they were formed from a distinct batch of mantle magma.

Based on geochemical considerations, about 80–95% crystallization of augite syenite magma must have occurred in order to reach the sodalite foyaite stage, which would require a huge underlying magma chamber (Engell 1973). Similarly, but even more extreme, Bailey et al. (1981) estimated about 99% fractionation of augite syenite required to reach the lujavrite stage. However, both calculations are based on the assumption that the trace element contents of the border facies of the augite syenite represent that of an actual melt, which is questionable.

Various dyke-rocks, some lujavrites and the relatively fine-grained rocks of the marginal pegmatite were proposed to represent the agpaitic stage of the Ilímaussaq magma (e.g., Larsen and Steenfelt 1974; Bailey et al. 1981; Sørensen 2006). The perhaps most promising candidate is the above-mentioned micro-kakortokite dyke (Larsen and Steenfelt 1974). Despite being highly evolved ($A.I. = 1.4$; $X_{Fe} = 0.98$) compared to the augite syenite ($A.I. = 0.8$; $X_{Fe} = 0.77$), this rock records the mineralogical evolution of the various Ilímaussaq units (for details see Marks and Markl 2003). Recent experimental work of Giehl et al. (2012, 2014) used the composition of this dyke as a model for the Ilímaussaq complex and simulated the liquid line of descent for peralkaline iron-rich phonolites. This work demonstrates that even strongly peralkaline melts can fractionate significant amounts of ol, aug, mag and alkfsp (representing augite syenite, a metaluminous and not peralkaline rock type), questioning the earlier assumption that augite syenite may represent a melt composition. We speculate that augite syenite could thus be a cumulate rock formed during the early evolutionary stages of a peralkaline melt. In some experiments, up to about 20% of this assemblage formed, corresponding roughly to the amount of augite syenite relative to agpaites we see today in the field. When the residual melts reach $A.I.$ values of about 2.4 or higher and are rich in chlorine (≥ 0.2 wt.%) and ZrO_2 (≥ 0.7 wt.%), aenigmatite, aegirine, eudialyte and sodalite become stable phases at about 800 °C (Giehl et al. 2014). Thus, this dyke rock may represent a melt composition that would be able to produce the phase assemblages seen in the Ilímaussaq rocks, allowing for the earlier fractionation of some olivine and augite. If this rock, however, separated from the Ilímaussaq source pool before, during or after the augite syenite stage remains questionable.

A Genetic Link Between Kakortokites and Naujaites?

Equally unclear are the detailed genetic relationships between naujaites and kakortokites. Naujaite contains large amounts of euhedral sodalite embedded in intersti-

tial alkali feldspar, nepheline, arfvedsonite, eudialyte and a number of accessories. Kakortokites are mineralogically very similar, but texturally very different. Eudialyte, nepheline, feldspar and arfvedsonite are euhedral cumulus phases and sodalite is only present in minor amounts in the lowermost part and diminishes upwards the kakortokite sequence (e.g., Sørensen and Larsen 1987).

A straightforward and intriguing idea would thus be that (parts of) the naujaite resemble the counterparts of the kakortokites with both rocks forming from the same magma batch (as Ussing already proposed in 1912). Since sodalite has the least density of the four minerals, it would float in a melt fastest. If sodalite saturation of the melt was achieved first and feldspar, nepheline, arfvedsonite and eudialyte would join the crystallizing assemblage slightly later, but still during an early magmatic stage, no amphibole-rich crystal mats (see above) acting as barriers would be present at this stage of magma evolution. Therefore, sodalite would not be hindered to float (except for maybe the lowermost crystallized sodalites, which may be captured in the lowermost exposed kakortokites, see above). A change from solely sodalite to a sodalite + feldspar + nepheline + eudialyte + arfvedsonite ± accessories cumulus assemblage could also account for the two geochemically distinct naujaite layers (see above; Krumrei et al. 2007). Large autoliths of naujaite are present in one specific unit of the kakortokites, demonstrating that parts of the naujaite were already consolidated when parts of the kakortokites were still forming (Bohse and Andersen 1981). This does not contradict the model above since both naujaite and kakortokites probably formed over a considerable time interval, giving enough time for such a process.

Larsen (1976) suggested that kakortokites crystallized from a magma that was distinct from the naujaite parent magma. This was based on the fact that amphiboles in the kakortokites are more magnesian and less calcic than those of the naujaite. As far more data are available today (Pfaff et al. 2008; Marks et al. 2004; Lindhuber et al. *in press*), the apparent difference in X_{Fe} is not present anymore. Although amphibole compositions from naujaite and kakortokite show considerable overlap, those from naujaite tend to be higher in Ca and Si (Fig. 14.9a). This, however can also be explained by the fact that in naujaite, amphibole is not a cumulus phase, but crystallized from interstitial melt captured in the rising sodalite mush and these small interstitial melt pockets are probably not representative of the whole magma column.

Preliminary numerical simulations (Baur 2012; Bons et al. 2015) show that it is possible to produce an uppermost light layer (sodalite-dominated), followed downwards by a rhythmic layered sequence (rich in alkali feldspar, eudialyte and amphibole), which is underlain by an amphibole-dominated unit (potentially represented by the “slumped kakortokites”?) out of one magma volume. Indeed, no unequivocal evidence for the detailed genetic relationships between naujaite and kakortokites is available to date and the final answer to this question is maybe hidden below the exposed lower layered kakortokites and critically depends on the interpretation of the proposed fault in the Lakseelv valley (Fig. 14.6; see Sect. “The Magmatic Evolution and Architecture of the Lujavrite Sill Complex”). Also, detailed knowledge on the spatial distribution and frequency of the early fayalite-hedenbergite-ulvöspinel assemblage (see Sect. “Major Mineralogical and Min-

eral Chemical Changes During the Magmatic to Hydrothermal Evolution of the Ilímaussaq System”) throughout the whole naujaite sequence (which is more than 600 m thick) could potentially help to test this hypothesis, but such a study has not been performed yet.

In all, there is no direct information on the actual melt compositions coexisting with the observed mineral assemblages—neither for the Ilímaussaq complex nor for the Gardar province in general, since to date, no melt inclusion study on the Ilímaussaq rocks or other Gardar rocks has been performed. Such a study would reveal many important details on the geochemical evolution and the liquid line of descent of the fascinating Ilímaussaq magmatic system.

Acknowledgements The funding of various Ilímaussaq- and Gardar-related projects provided by the Deutsche Forschungsgemeinschaft is gratefully acknowledged. Also, we highly appreciate the work of numerous student assistants, Diploma students, and PhD students, which together contributed to our mineralogical, petrological and geochemical knowledge on the Ilímaussaq area over the past 15 years. Special gratitude is owed to Thomas Wenzel. He provided critical support during microprobe work and brought many of the past Ilímaussaq projects to a success, because of his expertise, his steady interest in this work and his constructive comments on an earlier version of this manuscript (as well of several others in the past). Many constructive and fruitful discussions with numerous colleagues enhanced our understanding on the Gardar Province and the Ilímaussaq area. Amongst others we would like to thank Brian Upton, Henning Bohse and Paul Bons. We are also grateful to Salik Hard and co-workers of the Narsaq tourist office, Harry Andersen, Peter Lindberg, Helgi Jonasson and Stefán Magnússon, who provided logistic support during various field campaigns in South Greenland. We also thank Lotte Melchior Larsen, Tom Andersen and Troels F.D. Nielsen for their very detailed and constructive reviews, which helped us to improve the present work.

References

- Allaart JH (1969) The chronology and petrography of the Gardar dykes between Igaliko Fjord and Redekammen, South Greenland. *Rapp Grønl Geol Under* 25:26
- Allaart JH (1976) Ketilidian mobile belt in South Greenland. In: Escher A, Watt WS (eds) *Geology of Greenland*. Grønlands Geologiske Undersøgelse :121–151
- Andersen T, Sørensen H (2005) Stability of naujakasite in hyperagpaitic melts, and the petrology of naujakasite lujavrite in the Ilímaussaq alkaline complex, South Greenland. *Mineral Mag* 69:125–136
- Andersen S, Bohse H, Steenfelt A (1981) A geological section through the southern part of the Ilímaussaq intrusion. *Rapp Grønl Geol Undersøgelse* 103:39–42
- Andersen S, Bohse H, Steenfelt A (1988) Geological map of Greenland 1:20,000. The southern part of the Ilímaussaq complex, South Greenland. Grønlands Geologiske Undersøgelse/Geodætisk Institut, Denmark
- Andersen T, Friis H (submitted) The transition from agpaitic to hyperagpaitic magmatic crystallization in the Ilímaussaq alkaline complex, South Greenland. *J Petrol*
- Arzamastsev A, Arzamastseva L, Glaznev VN, Raevskii A (1998) Petrologic-geophysical model for the structure and composition of deep levels of the Khibina and Lovozero complexes, Kola Peninsula. *Petrology* 6:434–450
- Arzamastsev AA, Bea F, Glaznev VN, Arzamastseva LV, Montero P (2001) Kola alkaline province in the Paleozoic: evaluation of primary mantle magma composition and magma generation conditions. *Russ J Earth Sci* 3:1–32

- Bailey JC (1995) Cryptorhythmic and macrorhythmic layering in aegirine lujavrite, Ilimaussaq alkaline intrusion, South Greenland. *Bull Geol Soc Den* 42:1–16
- Bailey JC (2006) Geochemistry of boron in the Ilimaussaq alkaline complex, South Greenland. *Lithos* 91:319–330
- Bailey JC, Gwodzi R (1994) Li distribution in aegirine lujavrite, Ilimaussaq alkaline intrusion, South Greenland: role of cumulus and post-cumulus processes. *Lithos* 31:207–225
- Bailey JC, Rose-Hansen J, Løvborg L, Sørensen H (1981) Evolution of Th and U whole-rock contents in the Ilimaussaq intrusion. *Rapp Grønl Geol Undersøgelse* 103:87–98
- Bailey JC, Bohse H, Gwodzi R, Rose-Hansen J (1993) Li in minerals from the Ilimaussaq alkaline intrusion, South Greenland. *Bull Geol Soc Den* 40:288–299
- Bailey JC, Gwodzi R, Rose-Hansen J, Sørensen H (2001) Geochemical overview of the Ilimaussaq alkaline complex, South Greenland. *Geol Greenl Surv Bull* 190:35–53
- Bailey JC, Sørensen H, Andersen T, Kogarko LN, Rose-Hansen J (2006) On the origin of microrhythmic layering in arfvedsonite lujavrite from the Ilimaussaq alkaline complex, South Greenland. *Lithos* 91:301–318
- Baur A (2012) Modellierung von Schichtung in einer Magmenkammer durch Gravitationsortierung. Bachelorthesis, Universität Tübingen
- Beeskov B, Treloar PJ, Rankin AH, Vennemann TW, Spangenberg J (2006) A reassessment of models for hydrocarbon generation in the Khibina nepheline syenite complex, Kola Peninsula, Russia. *Lithos* 91:1–18
- Blaxland AB, van Breeman O, Steinfeldt A (1976) Age and origin of apgaitic magmatism at Ilimaussaq, South Greenland: Rb–Sr study. *Lithos* 9:31–38
- Bohse H, Andersen S (1981) Review of the stratigraphic divisions of the kakortokite and lujavrite in southern Ilimaussaq. *Rapp Grønl Geol Undersøgelse* 103:53–62
- Bohse H, Brooks CK, Kundendorf H (1971) Field observations on the Kakortokites of the Ilimaussaq intrusion, South Greenland, including mapping and analyses by portable x-ray fluorescence equipment for zirconium and niobium. *Rapp Grønl Geol Undersøgelse* 38:43
- Bons PD, Baur A, Elburg MA, Lindhuer MJ, Marks MAW, Soesoo A, van Milligen BP, Walte NP (2015) Layered intrusions and traffic jams. *Geology*. 43:71–74
- Botcharnikov RE, Koepke J, Holtz F, McCammon C, Wilke M (2005) The effect of water activity on the oxidation and structural state of Fe in a ferro-basaltic melt. *Geochim Cosmochim Acta* 69:5071–5085
- Bridgwater D, Coe K (1970) The role of stoping in the emplacement of the giant dikes of Isortoq, South Greenland. *Geol J Special issue* 2:67–78
- Bridgwater D, Harry WT (1968) Anorthosite xenoliths and plagioclase megacrysts in Precambrian intrusions of South Greenland. *Medd om Grønl* 185:243
- Derrey I (2012) Element transport and mineral replacement reactions during alkali contact metamorphism: effects on the Julianeåb granite induced by the Ilimaussaq intrusion, SW-Greenland. Diplomathesis, Universität Tübingen
- Eales HV, Cawthorn RG (1996) The Bushveld Complex. In: Cawthorn RG (Ed) Layered intrusions. Elsevier Science Ltd, Amsterdam, pp 181–230
- Emeleus CH, Upton BGJ (1976) The Gardar period in Southern Greenland. In: Escher A, Watt WS (eds) *Geology of Greenland. Grønlands Geologiske Undersøgelse* :152–181
- Emeleus CH, Cheadle MJ, Hunter RH, Upton BGJ, Wadsworth WJ (1996) The rum layered suite. In: Cawthorn RG (ed) Layered intrusions. Elsevier Science Ltd, Lausanne, pp 403–440
- Engell J (1973) A closed system crystal-fractionation model for the apgaitic Ilimaussaq intrusion, South Greenland, with special reference to the lujavrites. *Bull Geol Soc Den* 22:334–362
- Engell J, Hansen J, Jensen M, Kundendorf H, Løvborg L (1971) Beryllium mineralization in the Ilimaussaq Intrusion, South Greenland, with description of a field beryllometer and chemical methods. *Rapp Grønl Geol Undersøgelse* 33:40
- Féménias O, Coussaert N, Brassiness S, Demaiffe D (2005) Emplacement processes and cooling history of layered cyclic unit II-7 from the Lovozero alkaline massif (Kola Peninsula, Russia). *Lithos* 83:371–393

- Ferguson J (1964) Geology of the Ilímaussaq alkaline intrusion, South Greenland. *Bull Grøn Geol Undersøgelse* 39:82
- Ferguson J (1970) The significance of the kakortokite in the evolution of the Ilímaussaq intrusion, South Greenland. *Bull Grøn Geol Undersøgelse* 89:193
- Forsberg R, Rasmussen KL (1978) Gravity and rock densities in the Ilímaussaq area, South Greenland. *Rapp Grøn Geol Undersøgelse* 90:81–84
- Galakhov A (1975) Petrology of the Khibina alkaline massif. Nauka, Leningrad, 296 pp
- Garde AA, Hamilton MA, Chadwick B, Grocott J, McCaffrey KJW (2002) The Ketilidian orogen of South Greenland: geochronology, tectonics, magmatism, and fore-arc accretion during Palaeoproterozoic oblique convergence. *Can J Earth Sci* 39:765–793
- Gaweda A, Szopa K (2011) The origin of magmatic layering in the high tatra granite, Central Western Carpathians-implications for the formation of granitoid plutons. *Trans Royal Soc of Edinb* 102:129–144
- Giehl C, Marks MAW, Nowak M (2012) Phase relations and liquid lines of descent of an iron-rich peralkaline phonolitic melt: an experimental study. *Contrib Mineral Petrol* 165:283–304
- Giehl C, Marks MAW, Nowak M (2014) An experimental study on the influence of fluorine and chlorine on phase relations in peralkaline phonolitic melts. *Contrib Mineral Petrol* 167:977
- Giuli C, Alonso-Mori R, Cicconi MR, Paris E, Glatzel P, Eeckhout SG, Scaillet B (2012) Effect of alkalis on the Fe oxidation state and local environment in peralkaline rhyolitic glasses. *Am Mineral* 97:468–475
- GMEL (2015) Greenland minerals and energy Ltd. <http://www.ggg.gl>. Accessed 15 Feb 2015
- Goodenough KM, Upton BGJ, Ellam RM (2002) Long-term memory of subduction processes in the lithospheric mantle: evidence from the geochemistry of basic dykes in the Gardar Province of South Greenland. *J Geol Soc London* 159:705–714
- Graser G, Markl G (2008) Ca-rich ilvaite-epidote-hydrogarnet endoskarns: a record of late-magmatic fluid influx into the perisodic Ilímaussaq complex, South Greenland. *J Petrol* 49:239–265
- Graser G, Potter J, Köhler J, Markl G (2008) Isotope, major, minor and trace element geochemistry of late-magmatic fluids in the peralkaline Ilímaussaq intrusion, South Greenland. *Lithos* 106:207–221
- Halama R, Waight T, Markl G (2002) Geochemical and isotopic zoning patterns of plagioclase megacrysts in gabbroic dykes from the Gardar Province, South Greenland: implications for crystallisation processes in anorthositic magmas. *Contrib Mineral Petrol* 144:109–127
- Halama R, Wenzel T, Upton BGJ, Siebel W, Markl G (2003) A geochemical and Sr–Nd–O isotopic study of the Proterozoic Eriksfjord Basalts, Gardar Province, South Greenland: reconstruction of an OIB-signature in crustally contaminated rift-related basalts. *Mineral Mag* 67:831–853
- Halama R, Marks MAW, Brüggemann GE, Siebel W, Wenzel T, Markl G (2004) Crustal contamination of mafic magmas: evidence from a petrological, geochemical and Sr–Nd–Os–O isotopic study of the Proterozoic Isortoq dike swarm, South Greenland. *Lithos* 74:199–232
- Hamilton EI (1964) The geochemistry of the northern part of the Ilímaussaq intrusion, S.W. Greenland. *Bull Grøn Geol Undersøgelse* 42:104
- Hettmann K, Wenzel T, Marks MAW, Markl G (2012) The sulfur speciation in S-bearing minerals: new constraints by a combination of electron microprobe analysis and DFT calculations with special reference to sodalite-group minerals. *Am Mineral* 97:1653–1661
- Hettmann K, Marks MAW, Kreissig K, Zack T, Wenzel T, Rehkämper M, Jacob DE, Markl G (2014) The geochemistry of Tl and its isotopes during magmatic and hydrothermal processes: the peralkaline Ilímaussaq complex, southwest Greenland. *Chem Geol* 366:1–13
- Holloway JR, Jakobsson S (1986) Volatile solubilities in magmas: transport of volatiles from mantles to planet surface. *J Geophys Res* 91:D505–D508
- Kaliwoda M, Marschall H, Marks MAW, Ludwig T, Altherr R, Markl G (2011) Lithium, beryllium, boron and boron isotope systematics in the peralkaline Ilímaussaq intrusion (South Greenland) and its granitic country rocks: interplay between magmatic and hydrothermal processes. *Lithos* 125:51–64
- Karup-Møller S (1978) The ore minerals of the Ilímaussaq intrusion: their mode of occurrence and their conditions of formation. *Bull Grøn Geol Undersøgelse* 127:51

- Karup-Møller S, Rose-Hansen J (2013) New data on eudialyte decomposition minerals from karkortokites and associated pegmatites of the Ilímaussaq complex, South Greenland. *Bull Geol Soc Den* 61:47–70
- Karup-Møller S, Rose-Hansen J, Sørensen H (2010) Eudialyte decomposition minerals with new hitherto undescribed phases from the Ilímaussaq complex, South Greenland. *Bull Geol Soc Den* 58:75–88
- Khomyakov A (1995) Mineralogy of hyperagpaitic alkaline rocks. Scientific Publications, Clarendon, Oxford, p 222
- Kogarko LN (1977) Problems of the genesis of agpaitic magmas. Nauka, Moscow, p 294
- Kogarko LN, Krigmann LD (1970) Phase equilibria in the system nepheline-NaF. *Geochem Int* 7:103–107
- Kogarko LN, Romanchev BP (1983) Phase equilibria in alkaline melts. *Int Geol Rev* 25:534–546
- Köhler J, Schönenberger J, Upton B, Markl G (2009) Halogen and trace-element geochemistry in the Gardar Province, South Greenland: subduction-related metasomatism and fluid exsolution from alkalic melts. *Lithos* 113:731–747
- Konnerup-Madsen J (1980) Fluid inclusions in minerals from igneous rocks belonging to Precambrian continental Gardar rift province, South Greenland: the alkaline Ilímaussaq intrusion and the alkali acidic igneous complexes. PhD Thesis, University of Copenhagen 140 pp
- Konnerup-Madsen J (1984) Composition of fluid inclusions in granites and quartz syenites from the gardar continental rift province (South Greenland). *Bull Minéral* 107:327–340
- Konnerup-Madsen J (2001) A review of the composition and evolution of hydrocarbon gases during solidification of the Ilímaussaq alkaline complex, South Greenland. *Geol Greenl Surv Bull* 190:159–166
- Konnerup-Madsen J, Rose-Hansen J (1982) Volatiles associated with alkaline igneous rift activity: fluid inclusions in the Ilímaussaq intrusion and the Gardar granitic complexes (South Greenland). *Chem Geol* 37:79–93
- Konnerup-Madsen J, Rose-Hansen J (1984) Composition and significance of fluid inclusions in the Ilímaussaq peralkaline granite, South Greenland. *Bull Minéral* 107:317–326
- Konnerup-Madsen J, Larsen E, Rose-Hansen J (1979) Hydrocarbon-rich fluid inclusions in minerals from the alkaline Ilímaussaq intrusion, South Greenland. *Bull Minéral* 102:642–653
- Konnerup-Madsen J, Rose-Hansen J, Larsen E (1981) Hydrocarbon gases associated with alkaline igneous activity: evidence from compositions of fluid inclusions. *Rapp Grøn Geol Undersøgelse* 103:99–108
- Konnerup-Madsen J, Dubessy J, Rose-Hansen J (1985) Combined Raman microprobe spectrometry and microthermometry of fluid inclusions in minerals from igneous rocks of the Gardar Province (South Greenland). *Lithos* 18:271–280
- Konnerup-Madsen J, Kreulen R, Rose-Hansen J (1988) Stable isotope characteristics of hydrocarbon gases in the alkaline Ilímaussaq complex, South Greenland. *Bull Minéral* 111:567–576
- Kramm U, Kogarko LN (1994) Nd and Sr isotope signatures of the Khibina and Lovozero agpaitic centres, Kola Province, Russia. *Lithos* 32:225–242
- Krumrei TV, Villa IM, Marks MAW, Markl G (2006) A $^{40}\text{Ar}/^{39}\text{Ar}$ and U/Pb isotopic study of the Ilímaussaq complex, South Greenland: implications for the ^{40}K decay constant and for the duration of magmatic activity in a peralkaline complex. *Chem Geol* 227:258–273
- Krumrei TV, Pernicka E, Kaliwoda M, Markl G (2007) Volatiles in a peralkaline system: abiogenic hydrocarbons and F–Cl–Br systematics in the naujaite of the Ilímaussaq intrusion, South Greenland. *Lithos* 95:298–314
- Laier T, Nytoft HP (2012) Bitumen biomarkers in the mid-Proterozoic Ilímaussaq intrusion, Southwest Greenland—a challenge to the mantle gas theory. *Mar Petrol Geol* 30:50–65
- Larsen LM (1976) Clinopyroxenes and coexisting mafic minerals from the alkaline Ilímaussaq intrusion, South Greenland. *J Petrol* 17:258–290
- Larsen JG (1977a) Petrology of the late lavas of the Eriksfjord formation, Gardar Province, South Greenland. *Medd om Grøn* 53:31
- Larsen LM (1977b) Aenigmatites from the Ilímaussaq intrusion, South Greenland: chemistry and petrological implications. *Lithos* 10:257–270

- Larsen LM (1981) Chemistry of feldspars in the Ilímaussaq augite syenite with additional data on some other minerals. *Rapp Grøn Geol Unders* 103:31–37
- Larsen LM, Sørensen H (1987) The Ilímaussaq intrusion-progressive crystallization and formation of layering in an agpaite magma. In: Fitton JG, Upton, BGG (eds) *Alkaline igneous rocks*, Geological Society of London, Special Publication 30:473–488
- Larsen LM, Steenfelt A (1974) Alkali loss and retention in an iron-rich peralkaline phonolite dyke from the Gardar Province, South Greenland. *Lithos* 7:81–90
- Lauder W (1964) Mat formation and crystal settling in magma. *Nature* 202:1100–1101
- Lindhuber M, Marks MAW, Bons PD, Wenzel T, Markl G (in press) Crystal mat-formation as an igneous layering-forming process: textural and geochemical evidence from the ‘lower layered’ nepheline syenite sequence of the Ilímaussaq complex, South Greenland. *Lithos*
- Linnen RL, Keppler H (2002) Melt composition control of Zr/Hf fractionation in magmatic processes. *Geochim Cosmochim Acta* 66:3293–3301
- Mann U, Marks MAW, Markl G (2006) Influence of oxygen fugacity on mineral compositions in peralkaline melts: the Katzenbuckel volcano, Southwest Germany. *Lithos* 91:262–285
- Markl G (2001a) Stability of Na–Be minerals in late-magmatic fluids of the Ilímaussaq alkaline complex, South Greenland. *Geol Grøn Surv Bull* 190:145–158
- Markl G (2001b) A new type of silicate liquid immiscibility in peralkaline nepheline syenites (lujavrites) of the Ilímaussaq complex, South Greenland. *Contrib Mineral Petrol* 141:458–472
- Markl G, Baumgartner L (2002) pH changes in peralkaline late-magmatic fluids. *Contrib Mineral Petrol* 144:331–346
- Markl G, Marks MAW, Schwinn G, Sommer H (2001) Phase equilibrium constraints on intensive crystallization parameters of the Ilímaussaq complex, South Greenland. *J Petrol* 42:2231–2258
- Markl G, Marks MAW, Frost BR (2010) On the controls of oxygen fugacity in the generation and crystallization of peralkaline melts. *J Petrol* 51:1831–1847
- Marks MAW, Markl G (2001) Fractionation and assimilation processes in the alkaline augite syenite unit of the Ilímaussaq intrusion, South Greenland, as deduced from phase equilibria. *J Petrol* 42:1947–1969
- Marks MAW, Markl G (2003) Ilímaussaq ‘en miniature’: closed-system fractionation in an agpaite dyke rock from the Gardar Province, South Greenland. *Mineral Mag* 67:893–919
- Marks MAW, Vennemann TW, Siebel W, Markl G (2003) Quantification of magmatic and hydrothermal processes in a peralkaline syenite-alkali granite complex based on textures, phase equilibria, and stable and radiogenic isotopes. *J Petrol* 44:1247–1280
- Marks MAW, Vennemann T, Siebel W, Markl G (2004) Nd-, O-, and H-isotopic evidence for complex, closed-system fluid evolution of the peralkaline Ilímaussaq intrusion, South Greenland. *Geochim Cosmochim Acta* 68:3379–3395
- Marks MAW, Rudnick R, Vennemann T, McCammon C, Markl G (2007) Arrested kinetic Li isotope fractionation at the margin of the Ilímaussaq complex, South Greenland: evidence for open-system processes during final cooling of peralkaline igneous rocks. *Chem Geol* 246:207–230
- Marks MAW, Hettmann K, Schilling J, Frost BR, Markl G (2011) The mineralogical diversity of alkaline igneous rocks: critical factors for the transition from miaskitic to agpaite phase assemblages. *J Petrol* 52:439–455
- McBirney AR (1996) The Skaergaard intrusion. In: Cawthorn RG (ed) *Layered intrusions*. Elsevier Science Ltd, New York, pp 147–180
- McCallum IS (1996) The Stillwater complex. In: Cawthorn RG (ed) *Layered intrusions*. Elsevier Science Ltd, Oxford, pp 441–484
- Morse SA (1969) The Kiglapait layered intrusion, Labrador. *Geol Soc Am Memoir* 112:204
- Müller-Lorch D, Marks MAW, Markl G (2007) Na and K distribution in agpaite pegmatites. *Lithos* 95:315–330
- Mysen BO, Yamashita S (2010) Speciation of reduced C–O–H volatiles in coexisting fluids and silicate melts determined in-situ to ~1.4 GPa and 800 °C. *Geochim Cosmochim Acta* 74:4577–4588

- Namur O, Abily B, Boudreau A, Blanchette F, Bush JWM, Ceuleneer G, Charlier B, Donaldson CH, Duchesne JC, Higgins MD, Morata D, Nielsen TFD, O'Driscoll B, Pang KN, Peacock T, Spandler C, Toramaru A, Veksler I (2015) Igneous Layering in Basaltic Magma Chambers. In Charlier et al. (Editors) Layered Intrusions, Springer Geology, Dordrecht, in press. (DOI 10.1007/978-94-017-9652-1_2)
- Naslund HR, McBirney AR (1996) Mechanisms of formation of igneous layering. In: Cawthorn RG (ed) Layered intrusions. Elsevier Science Ltd, Shannon, pp 1–44
- Nielsen TF, Bernstein S (2009) Chemical variations in the triple group of the skaergard intrusion: insights for the mineralization and crystallization process. AGU Fall meeting 2009, Abstract V21A 1956
- Nielsen BL, Steenfelt A (1979) Intrusive events at Kvanefjeld in the Ilímaussaq igneous complex. *Bull Geol Soc Den* 27:143–155
- Nivin VA (2002) Gas concentrations in minerals with reference to the problem of the genesis of hydrocarbon gases in rocks of the Khibiny and Lovozero complexes. *Geochem Int* 40:883–898
- Nivin VA, Devirts AL, Lagutina YP (1995) The origin of the gas phase in the Lovozero massif based on hydrogen-isotope data. *Geochem Int* 32:65–71
- Nivin VA, Belov NI, Treloar PJ, Timofeyev VV (2001) Relationships between gas geochemistry and release rates and the geochemical state of igneous rock massifs. *Tectonophysics* 336:233–244
- Nivin VA, Treloar PJ, Konopleva NG, Ikorsky SV (2005) A review of the occurrence, form and origin of C-bearing species in the Khibiny alkaline igneous complex, Kola Peninsula, Russia. *Lithos* 85:93–112
- O'Driscoll B, Troll VR, Reavy RJ, Turner P (2006) The Great Euclid intrusion of Ardnamurchan, Scotland: reevaluating the ring-dike concept. *Geology* 34:189–192
- Parsons I (2012) Full stop for mother earth. *Elements* 8:396–398
- Paslick CR, Halliday AN, Davies GR, Mezger K, Upton BGJ (1993) Timing of proterozoic magmatism in the Gardar Province, southern Greenland. *Bull Geol Soc Am* 105:272–278
- Petersen OV (2001) List of minerals identified in the Ilímaussaq alkaline complex, South Greenland. *Geol Greenl Surv Bull* 190:25–34
- Petersilie IA, Sørensen H (1970) Hydrocarbon gases and bituminous substances in rocks from the Ilímaussaq alkaline intrusion, South Greenland. *Lithos* 3:59–66
- Pfaff K, Krumrei TV, Marks M, Wenzel T, Rudolf T, Markl G (2008) Chemical and physical evolution of the 'lower layered series' from the nepheline syenitic Ilímaussaq intrusion, South Greenland: implications for the origin of magmatic layering in peralkaline felsic liquids. *Lithos* 106:280–296
- Potter J, Konnerup-Madsen J (2003) A review of the occurrence and origin of hydrocarbons in igneous rocks. In: Petford N, McCaffrey KJW (eds) Hydrocarbons in crystalline rocks, Geological Society Special Publication 214:151–173
- Potter J, Longstaffe FJ (2007) A gas-chromatograph continuous flow isotope ratio mass-spectrometry method for ^{13}C and D measurement of complex fluid inclusion volatiles: examples from the Khibina alkaline igneous complex, Northwest Russia and the South Wales Coalfields. *Chem Geol* 244:186–201
- Potter J, Rankin AH, Treloar PJ (2004) Abiogenic Fischer-Tropsch synthesis of hydrocarbons in alkaline igneous rocks: fluid inclusion, textural and isotopic evidence from the Lovozero complex, N.W. Russia. *Lithos* 75:311–330
- Potter J, Rankin AH, Treloar PJ, Nivin VA, Ting W, Ni P (1998) A preliminary study of methane inclusions in alkaline igneous rocks of the Kola igneous province, Russia: implications for the origin of methane in igneous rocks. *Eur J Mineral* 10:1167–1180
- Poulsen V (1964) The sandstones of the Precambrian Eriksfjord formation in South Greenland. *Rapp Grønl Geol Under* 2:16
- Pupier E, Barbey O, Toplis M, Bussy F (2008) Igneous layering, fractional crystallization and growth of granitic plutons: the Dolbel Batholith in SW Niger. *J Petrol* 49:1043–1068

- Ratschbacher B, Marks MAW, Wenzel T, Bons P, Markl G (submitted) Emplacement and geochemical evolution of highly evolved nepheline syenites in the composite alkaline to peralkaline Ilímaussaq complex, SW Greenland. *Lithos*
- Rose-Hansen J, Sørensen H (2001) Minor intrusions of peralkaline microsyenite in the Ilímaussaq alkaline complex, South Greenland. *Bull Geol Soc Den* 48:9–29
- Rose-Hansen J, Sørensen H (2002) Geology of the Lujavrites from the Ilímaussaq alkaline complex South Greenland, with information from seven bore holes. *Medd om Grønl Geosci* 40:58
- Rønsbo JG (1989) Coupled substitutions involving REEs and Na and Si in apatites in alkaline rocks from the Ilímaussaq intrusion, South Greenland, and the petrological implications. *Am Mineral* 74:896–901
- Rønsbo JG (2008) Apatite in the Ilímaussaq alkaline complex: occurrence, zonation and compositional variation. *Lithos* 106:71–82
- Sass JH, Nielsen BL, Wollenberg HA, Munroe RJ (1972) Heat flow and surface radioactivity at two sites in South Greenland. *J Geophys Res* 77(32):6435–6444
- Schilling J, Wu F-Y, McCammon C, Wenzel T, Marks MAW, Pfaff K, Jacob DE, Markl G (2011) The compositional variability of eudialyte-group minerals. *Mineral Mag* 75:87–115
- Schmid C (2008) Die Pulaskite der Ilímaussaq Intrusion in Südgrönland. Diplomathesis, Universität Tübingen
- Schönenberger J, Marks M, Wagner T, Markl G (2006) Fluid-rock interaction on autoliths of agpaitic nepheline syenites in the Ilímaussaq intrusion, South Greenland. *Lithos* 91:331–351
- Scott HP, Hemley RJ, Mao HK, Herschbach DR, Fried LE, Howard WM, Bastea S (2004) Generation of methane in the Earth's mantle: in situ high pressure-temperature measurements of carbonate reduction. *PNAS* 101:14023–14026
- Sobolev AV, Bazarova TY, Shugorova NA, Bazarov LS, Dolgov YA, Sørensen H (1970) A preliminary examination of fluid inclusions in nepheline, sorensonite, tugtupite and chkalovite from the Ilímaussaq alkaline intrusion, South Greenland. *Bull Grønl Geol Under* 81:32
- Sørensen H (1962) On the occurrence of steenstrupine in the Ilímaussaq massif, Southwest Greenland. *Bull Grønl Geol Under* 32:251
- Sørensen H (1968) Rhythmic igneous layering in peralkaline intrusions: an essay review on Ilímaussaq (Greenland) and Lovozero (Kola, USSR). *Lithos* 2:261–283
- Sørensen H (1978) The position of the augite syenite and pulaskite in the Ilímaussaq intrusion, South Greenland. *Bull Geol Soc Den* 27:15–23
- Sørensen H (1992) Agpaitic nepheline syenites: a potential source of rare elements. *Appl Geochem* 7:417–427
- Sørensen H (1997) The agpaitic rocks—an overview. *Mineral Mag* 61:485–498
- Sørensen H (2001) Brief introduction to the geology of the Ilímaussaq alkaline complex, South Greenland, and its exploration history. *Geol Greenl Surv Bull* 190:7–24
- Sørensen H (2006) The Ilímaussaq alkaline complex, South Greenland—an overview of 200 years of research and an outlook. *Medd om Grønl Geosci* 45:10–31
- Sørensen H, Larsen LM (1987) Layering in the Ilímaussaq alkaline intrusion, South Greenland. In: Parsons I (ed) *Origins of igneous layering*. D. Reidel, Dordrecht, pp 1–28
- Sørensen H, Larsen LM (2001) The hyper-agpaitic stage in the evolution of the Ilímaussaq alkaline complex, South Greenland. *Geol Greenl Surv Bull* 190:83–94
- Sørensen H, Hansen J, Bondesen E (1969) Preliminary account of the geology of the Kvanefjeld area of the Ilímaussaq intrusion, South Greenland. *Rapp Grønl Geol Under* 18:40
- Sørensen H, Rose-Hansen J, Nielsen BL, Løvborg L, Sørensen E, Lundgaard T (1974) The uranium deposit at Kvanefjeld, the Ilímaussaq intrusion, South Greenland. *Rapp Grønl Geol Under* 60:54
- Sørensen H, Bailey JC, Kogarko LN, Rose-Hansen J, Karup-Møller S (2003) Spheroidal structures in arfvedsonite lujavrite, Ilímaussaq alkaline complex, South Greenland—an example of macro-scale liquid immiscibility. *Lithos* 70:1–20
- Sørensen H, Bohse H, Bailey JC (2006) The origin and mode of emplacement of lujavrites in the Ilímaussaq alkaline complex, South Greenland. *Lithos* 91:286–300

- Sørensen H, Bailey JC, Rose-Hansen J (2011) The emplacement and crystallization of the U–Th–REE-rich apgaitic and hyperapgaitic Iujavrites at Kvanefjeld, Ilimaussaq alkaline complex, South Greenland. *Bull Geol Soc Den* 59:69–92
- Steenfelt A (1981) Field relations in the roof zone of the Ilimaussaq intrusion with special reference to the position of the alkali acid rocks. *Rapp Grøn Geol Under* 103:43–52
- Stevenson R, Upton BGJ, Steenfelt A (1997) Crust-mantle interaction in the evolution of the Ilimaussaq complex, South Greenland: Nd isotopic studies. *Lithos* 40:189–202
- TANBREEZ (2014) TANBREEZ Mining Greenland A/S. <http://www.tanbreez.com>. Accessed 2 Aug 2014
- Thorning L, Stemp RW (1997) Projects Aeromag 1995 and Aeromag 1996. Results from aeromagnetic surveys over South Greenland (1995) and South-West and southern West Greenland (1996). *Dan Grøn Geol Under Rapp* 11:44
- Upton BGJ (1991) Gardar mantle xenoliths: Iglutalik, South Greenland. *Rapp Grøn Geol Under* 150:37–43
- Upton BGJ (2013) Tectono-magmatic evolution of the southern branch of the Gardar rift in the late Gardar period. *Geol Surv Den Greenl Bull* 29:124
- Upton BGJ, Emeleus CH (1987) Mid-Proterozoic alkaline magmatism in southern Greenland: the Gardar Province. In: Fitton JG, Upton BGJ (eds) *Alkaline igneous rocks*, Geological Society of London, Special Publication 30:449–471
- Upton B, Pulvertaft TCR (1961) Textural features of some contrasted igneous cumulates from South Greenland. *Medd om Grøn* 123:1–29
- Upton BGJ, Martin AR, Stephenson D (1990) Evolution of the tugtutôq central complex, South Greenland; a high-level, rift-axial, late-Gardar centre. *J Volcanol Geotherm Res* 43:195–214
- Upton BGJ, Parsons I, Emeleus CH, Hodson M (1996) Layered alkaline igneous rocks of the Gardar Province, South Greenland. In: Cawthorn RG (ed) *Layered intrusions*. Elsevier Science Ltd, Tokyo, pp 331–364
- Upton BGJ, Emeleus CH, Heaman LM, Goodenough KM, Finch A (2003) Magmatism of the mid-Proterozoic Gardar Province, South Greenland: chronology, petrogenesis and geological setting. *Lithos* 68:43–65
- Ussing NV (1912) Geology of the country around Julianehaab, Greenland. *Medd om Grøn* 38:426
- Vlasov K, Kuzmenko M, Eskova E (1966) The Lovozero alkali massif. Oliver and Boyd, Edinburgh, p 627
- Waight T, Baker J, Willigers B (2002) Rb isotope dilution analyses by MC-ICPMS using Zr to correct for mass fractionation: towards improved Rb–Sr geochronology? *Chem Geol* 186:99–116
- Watson EB (1979) Zircon saturation in felsic liquids: experimental results and applications to trace element geochemistry. *Contrib Mineral Petrol* 70:407–419
- Wilson AH (1996) The Great Dyke of Zimbabwe. In: Cawthorn RG (ed) *Layered intrusions*. Elsevier Science Ltd, pp 365–402
- Zhang C, Duan Z (2010) A model for C–O–H fluid in the Earth’s mantle. *Geochim Cosmochim Acta* 73:2089–2102
- Zhang T, Kross BM (2001) Experimental investigation on the carbon isotope fractionation of methane during gas migration by diffusion through sedimentary rocks at elevated temperature and pressure. *Geochim Cosmochim Acta* 65:2723–2742
- Zirner ALK, Marks MAW, Wenzel T, Jacob DE, Markl G (submitted) Rare earth elements in apatite as a monitor of crystallization and metasomatic processes: the Ilimaussaq intrusion, South Greenland, as a type example. *Lithos*